Durham Research Online

On the Formation of Globular Cluster Systems in a Hierarchical Universe

M.A. Beasley,[1]* C.M. Baugh,[2] Duncan A. Forbes,[1] R.M. Sharples,[2] C.S. Frenk[2]

[1] *Centre for Astrophysics & Supercomputing, Swinburne University of Technology, Hawthorn, VIC 3122, Australia.*
[2] *Department of Physics, University of Durham, Durham DH1 3LE, UK.*

arXiv:astro-ph/0202191v1 9 Feb 2002

ABSTRACT

We have investigated the formation of globular cluster (GC) systems in the fiducial semi-analytic model of galaxy formation of Cole et al., by assuming that GCs are formed at high-redshift ($z > 5$) in proto-galactic fragments, and during the subsequent gas-rich merging of these fragments. Under these assumptions we have simulated the GC systems of 450 elliptical galaxies, and find that the majority (93 %) are intrinsically bimodal in metallicity. We find that, in the mean, the metal-rich GC sub-populations are younger than the metal-poor GC sub-populations, with ages of 9 Gyr and 12 Gyr respectively, and that the mean ages of the metal-rich GCs are dependent upon host galaxy luminosity and environment (halo circular velocity), whereas the metal-poor GCs are not. We find that the continued gaseous merging of the proto-galactic fragments leads to significant age-structure amongst the metal-rich GCs. These GCs exhibit a large age-range (5 to 12 Gyr), which increases for low-luminosity galaxies, and for galaxies in low circular velocity haloes. Moreover, the metal-rich GCs associated with low-luminosity field and/or group ellipticals, are ~ 2 Gyr younger than the metal-rich GCs in luminous cluster ellipticals. We find the total GC populations scale with host galaxy luminosity as $N_{\rm GC} \propto L_{V,{\rm gal}}^{1.25}$, a result in agreement with observations of luminous elliptical galaxies. This scaling is due to a systematic increase in the $\mathcal{M}/\mathcal{L}$ ratios of the galaxy haloes with luminosity for $L_{V,{\rm gal}} > L_*$ galaxies in the model. A comparison between the luminosity growth of the model ellipticals and their GC formation indicates that mergers do not significantly effect S_N at $z < 2$. We find the mean colours of the both the metal-rich and metal-poor GCs exhibit only a weak dependence upon host galaxy luminosity, a result consistent with contemporary observations. We conclude that gaseous merging, the bulk of which occurs at $1 \leq z \leq 4$ in our ΛCDM model, leads to the formation of the metal-rich peak of the GC systems of elliptical galaxies. We suggest that the formation and subsequent truncation of the metal-poor GCs in the proto-galactic fragments is closely related to the star formation rate in these fragments, which may have been significantly higher at very early times.

Key words: galaxies: star clusters– galaxies: formation – galaxies: evolution – galaxies: elliptical and lenticular, cD

1 INTRODUCTION

Globular clusters (GCs) are a seemingly ubiquitous feature of nearly all galaxies in the local Universe. A growing body of evidence has indicated the presence of correlations between GC systems and their host galaxies, such as the mean metallicity of GC systems (e.g. Brodie & Huchra 1991) and the total number of GCs with host galaxy luminosity (e.g. Djorgovski & Santiago 1992; Zepf, Geisler, & Ashman

1994) or cluster velocity dispersion (e.g. Blakeslee, Tonry, & Metzger 1997). Results such as these suggest that GC formation is intimately linked to galaxy star formation, and since GCs are simpler stellar systems than galaxies, they provide a unique record of the formation history of their host galaxy.

In the past decade, there have been two key advances in GC research. One has been the discovery of newly forming, massive young star clusters (YMCs to use the terminology of Larsen & Richtler 1999), with masses and sizes consistent with those expected for newly formed GCs. Such YMCs are seen to be forming in a variety of star-bursting environments (Meurer et al. 1995) including violent galaxy merg-

---

* email: mbeasley@astro.swin.edu.au

ers (e.g. Holtzman et al. 1992; Whitmore & Schweizer 1995; Schweizer et al. 1996; Zepf et al. 1999; Forbes & Hau 2000), star-bursts (e.g. O'Connell, Gallagher, & Hunter 1994; Watson et al. 1996), circum-nuclear ring galaxies (Barth et al. 1995) and the discs of otherwise unperturbed spirals (Larsen & Richtler 1999). The inference is that YMCs can form in a wide variety of galactic environments.

The second development has been the discovery of bimodality in the broad-band colours of many (perhaps most) GC systems (e.g. Zepf & Ashman 1993; Elson, Santiago, & Gilmore 1996; Geisler, Lee, & Kim 1996; Forbes, Brodie, & Huchra 1997; Gebhardt & Kissler-Patig 1999; Kundu & Whitmore 2001; Larsen et al. 2001). Owing to the relative insensitivity of broad-band colours to age differences in old stellar populations (O'Connell 1976; Worthey 1994) these bimodal colour distributions in GC systems are, by implication, thought to largely reflect bimodal metallicity distributions. Spectroscopic metallicities obtained for the Milky Way (see Carney & Harris 2001), M31 (Barmby et al. 2000) and several giant ellipticals (e.g. Cohen, Blakeslee, & Ryzhov 1998; Kissler-Patig et al. 1998; Beasley et al. 2000; Forbes et al. 2001) largely support this notion.

The metallicity bimodality of the GC systems in luminous ellipticals was predicted by Ashman & Zepf (1992), who presented a model for the formation of metal-rich GCs during the merging of gas-rich spirals. Subsequent ideas have also been developed which attempt to explain the bimodality (and other properties) of GC systems, *in-situ*, multi-phase collapse (Forbes, Brodie, & Grillmair 1997; Harris, Harris, & McLaughlin 1998) and the accretion of dwarf galaxies and their GCs (Cote, Marzke, & West 1998). Whilst all of these models have been successful in explaining certain properties of GC systems, in detail each has its problems (see Carney & Harris 2001 for details). However, rather than (somewhat artificially) separating these models, it is perhaps more reasonable to expect a hybrid of some or all of the above scenarios. In this respect, 'semi-analytic' models of galaxy formation may offer a suitable framework within which to achieve such a hybrid model in a more natural way.

Semi-analytic models of galaxy formation have proved themselves to be valuable tools with which to follow the formation and subsequent evolution of galaxies in hierarchical clustering cosmologies (e.g. White & Rees 1978; White & Frenk; Kauffmann, White, & Guiderdoni 1993; Cole et al. 1994). These models treat the galaxy formation problem in an *ab initio* fashion. Starting from a power spectrum of primordial density fluctuations, the merger history and assembly of dark matter haloes is computed. The properties of the galaxy population are then calculated through to the present day using simple, physically motivated analytic recipes to follow the evolution of gas and stars.

The parameters and input physics of the semi-analytic models are constrained by the requirement that the models should match various 'fundamental' galaxy properties, and these constraints vary between the different groups. Such properties include the local B and K-band galaxy luminosity functions, the relative fractions of galaxy morphological types, the slope of the Tully-Fisher relation and the gas fractions in discs in the case of the model used in this paper (e.g. Cole et al. 1994; 2000; Baugh, Cole, & Frenk 1996; 1998), or the zero-point of the Tully-Fisher relation and the slope of the galaxy colour-magnitude relation in the case of
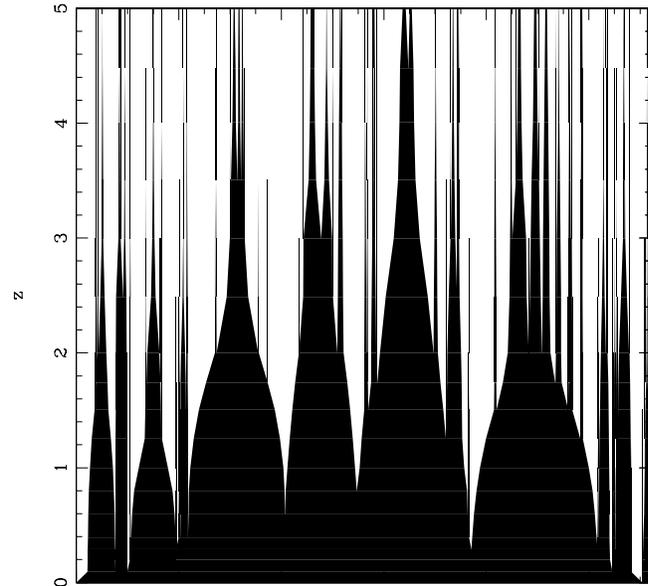

Figure 1. Merger tree for an elliptical galaxy of mass $\sim 2.3 \times 10^{11}$ M$_\odot$, beginning at redshift 5, and proceeding up to the present day. The width of the 'branches' reflect mass at a given epoch. The merger tree has been normalised to possess unit width at $z = 0$.

the Munich and Santa Cruz groups (e.g. Kauffmann, White, & Guiderdoni 1993; Kauffmann & Charlot 1998; Somerville & Primack 1999). The resulting model predictions are then compared to other observed galaxy properties.

Currently, none of the semi-analytic models have been tested in any detail against the growing wealth of data on GC systems of galaxies. Here, for the first time, we compare expectations from the fiducial semi-analytic model of Cole et al. (2000) with the observed properties of GC systems.

The layout of this paper is as follows: in Section 2 we describe the semi-analytic model used in this study and how we go about producing GC systems from the star formation histories it produces. In Section 3 we show examples of the resulting GC systems of individual galaxies and compare them with observations of GC systems. Next, in Section 4, we compare the global properties of our model GC systems with a compilation of contemporary observational data for the GC systems of early-type galaxies. In Section 5 we discuss some of the principal issues raised in this study, before presenting a summary and our conclusions from this work in Section 6.

2 METHODOLOGY

2.1 The Semi-Analytic Model

The semi-analytic model we use in this study is the GALFORM code (Cole et al. 2000). A wide range of physical processes are incorporated in this model; here we give only a brief outline of the model and refer the reader to Cole et al. (2000) for a complete description.

The GALFORM model used in this paper is the fiducial

ΛCDM model of Cole et al.(2000), with the following values of the cosmological parameters: a mean mass density, $\Omega_0 = 0.3$, a cosmological constant, $\Lambda_0 = 0.7$, a Hubble constant of $h = 0.7$ (where $H_0 = 100\ h\ \mathrm{kms}^{-1}\,\mathrm{Mpc}^{-1}$) and a linear variance in spheres of radius $8h^{-1}\mathrm{Mpc}$ of $\sigma_8 = 0.93$. Once the cosmological parameters and the form of the power spectrum of density fluctuations have been specified, the full merger history of an ensemble of dark matter haloes is computed using the Monte-Carlo prescription described in Cole et al.(2000) (see also Baugh et al. 1998).

The semi-analytic code utilises a set of simple rules to to model the complex physics of galaxy formation. The processes treated include: *(i)* The shock heating of gas in the gravitational potential wells of dark matter haloes. *(ii)* The subsequent radiative cooling of this gas, tracking the angular momentum of the gas distribution. *(iii)* The formation of stars from the cooled gas. *(iv)* Feedback processes, e.g. stellar winds and supernovae, that re-heat some of the cooled gas and thereby regulate the star formation rate. *(v)* The chemical evolution of the various reservoirs of gas and stars (see Fig. 3 of Cole et al. 2000). *(vi)* Mergers of galaxies inside a common dark matter halo, based upon dynamical friction arguments. Bursts of star formation can occur during a merger if cold gas is present. *(vii)* The evolution of the stellar populations of galaxies. The extinction of starlight is computed in a self-consistent way using the chemical evolution model and the size of the disk and bulge components. We note that Benson et al. (2001a) describe extensions to the scheme of Cole et al.(2000), refining the treatment of the cooling of gas in relatively small dark matter haloes at high redshift and improving the calculation of merger timescales. These features are not used in the model presented here. For bright galaxies at reasonable redshifts, we expect that these two versions of the GALFORM code will produce comparable predictions.

We show an example of the evolutionary history of a GALFORM galaxy in Figure 1 (see Baugh, Cole, & Frenk 1996, Baugh et al. 1998). The figure shows the formation and evolution of the progenitors of a present day massive elliptical galaxy. The width of the filled regions indicates the fraction of the present day galaxy's stellar mass that is contributed by each progenitor. In the case of Figure 1, the progenitors of this elliptical galaxy experienced several fairly significant mergers that would lead to a dramatic change in the progenitors' morphology (e.g. at redshifts 0.8 and 0.3), and numerous minor mergers.

Star formation in the discs of the progenitors of present day galaxies provides the source of metal-poor GCs in our model (see next section). When we say GCs are formed in gas discs, this does *not* mean that the metal-poor GCs are associated with the stellar/gas discs of spiral galaxies. Rather that the origin of the metal-poor GCs are protogalactic cold-gas discs modelled in GALFORM. Henceforth, to distinguish between galaxy discs and the proto-galactic discs modelled in GALFORM, we abbreviate the latter to *PGDs*.

We show the evolution of the mean ratio of cold gas to stars in the PGDs of a present-day elliptical in Figure 2. At redshift ~ 5, the majority of these PGDs have a high mass fraction of cold gas ($\sim 95\%$). It is only at $z \sim 0.6$ that this ratio reaches unity, as gas is used up during star formation.

In addition to star formation in PGDs, bursts of star formation can accompany galaxy mergers. Galaxies merge
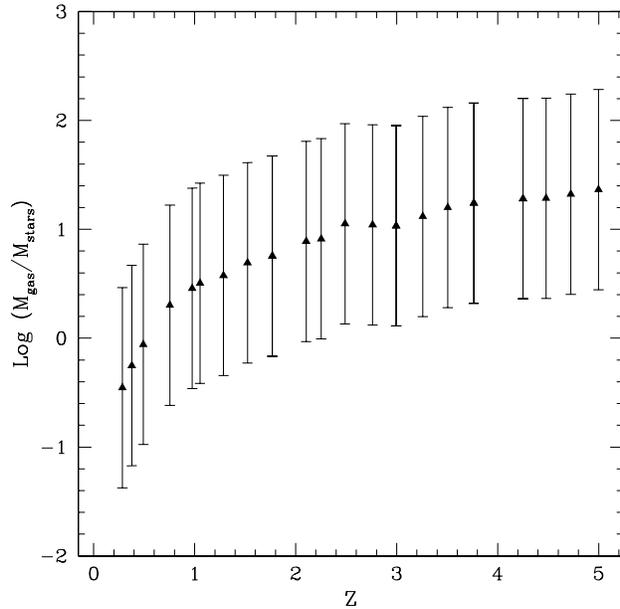

Figure 2. Mean ratio of the mass in cold gas to stars for the progenitor PGDs for a present day elliptical in the semi-analytic model. Filled triangles with error-bars represent mean values with their associated 10 and 90 percentiles of the distribution. The cold gas-fractions with respect to stars range from $\sim 95\%$ at $z = 5$, to $\sim 10\%$ at $z = 0$.

in the model if the timescale for a galaxy orbit to decay to the centre of a dark matter halo, as a result of dynamical friction, is shorter than the lifetime of the halo, which we take to be the time for the halo to double its mass through the accretion and mergers of smaller subunits. If the mass of the satellite is larger than 30% of the mass of the central galaxy, then the merger is designated as a major merger (see Kauffmann, White, & Guiderdoni 1993; Baugh, Cole, & Frenk1996). In this case, if cold gas is present then a burst of star formation takes place. Thus it can be seen that the morphology of a galaxy in GALFORM is essentially a function of time. In a major merger, any stellar discs in the merging galaxies are destroyed and the resulting galaxy will be bulge dominated, i.e. it will be early-type. Over time, in the absence of additional major mergers, gas will cool and the bulge will accrete a disc of enriched, cold gas, thus forming a spiral (or lenticular) galaxy. An important point to bear in mind when considering this model is that much of the star formation occurs at relatively low redshift, with only $\sim 50\ \%$ of stars forming prior to redshifts of $z \sim 1.5$. This occurs because the formation of stars in lower mass haloes is suppressed by feedback from star formation.

2.2 Star Formation Histories to Globular Clusters

2.2.1 Forming Globular Clusters

Our goal is to create a simple model for forming GC systems within GALFORM, thereby keeping the number of new parameters required to a minimum. However, in creating GC systems from the star formation histories (SFHs) produced in the model, requires us to make several assumptions

about the nature of GC formation and how this relates to the global star formation in a galaxy. Our principal assumption is that GC formation accompanies the two modes of star formation. We assume that GCs form: *(i)* contemporaneously with the star formation occurring in PGDs and *(ii)* during major mergers involving star formation.

The GCs formed in both modes become the composite GC system of the resulting galaxy. As we show later, this can result in two sub-populations of GCs which have undergone different levels of chemical enrichment; one metal-poor GC sub-population, formed in cold gas PGDs, and one metal-rich formed during gas-rich merging. Henceforth, in order to distinguish between the GC sub-populations, we refer to the PGD-formed GCs as *blue* GCs and the merger-formed GCs as *red* GCs.

For each model realisation, we build the GC system of each galaxy by assuming that some fraction of the stars formed remain in a clustered mode, i.e. they become, and remain, GCs. We calculate total numbers of GCs (since we do not have explicit luminosity information), and adopt a mean GC mass, $\langle M_{\rm GC} \rangle$, corresponding to that of the Milky Way GC system of $\sim 3.0 \times 10^5 {\rm M}_\odot$ (from the McMaster catalogue of Harris 1996; May 15th, 1997 version).

We neglect the possible effects of the dynamical evolution and destruction of the GCs, which may be significant (e.g. Aguilar, Hut, & Ostriker 1988; Gnedin & Ostriker 1997). The study of McLaughlin (1999) suggests that the total mass of GC systems is not significantly effected by the dynamical destruction of low-mass GCs within an effective radius of an elliptical. However, the simulations of Vesperini (2000) indicate that some 10–20% of the initial GC system of a luminous elliptical may be destroyed over a Hubble time due to dynamical destruction processes.

Subsequently, we define a 'formation efficiency' of the GCs as the mass of GCs which form and survive the possible effects of dynamical destruction ($M_{\rm GC}$) relative to the mass of stars which form and survive ($M_{\rm stars}$) associated with the model galaxies:

$$\epsilon \equiv \frac{M_{\rm GC}}{M_{\rm stars}} \qquad (1)$$

it is effectively this efficiency – the fraction of GCs that are formed and survive with respect to stars – which is measured when one obtains the 'specific frequency' (S_N) of a galaxy, as discussed further in § 4.1.

Under the hypothesis that *no* dynamical destruction of the GCs operates, this efficiency may be directly equated to a global formation efficiency for the GCs. If, however, GC systems truly undergo significant dynamical destruction (e.g. Vesperini 2000), then ϵ is more a reflection of a GC 'survival efficiency'.

With our stated assumptions, we construct GC systems for each galaxy as follows: for each galaxy merger tree, GALFORM outputs SFHs for stars formed both in PGDs and in bursts, yielding stellar masses, hot gas mass, cold gas mass and metallicities (Z) as a function of look-back time. To create the blue GCs, we take a fraction of the cumulative total of stars formed in the PGDs, dictated by $M_{\rm GC}$ and our adopted blue GC formation efficiency ($\epsilon_{\rm blue}$). This yields age and metallicity distributions for the metal-poor GCs as a function of redshift.

For each major merger, red GCs are created correspond-

ing to our adopted red GC formation efficiency ($\epsilon_{\rm red}$), providing that a high enough mass of stars are formed in the burst ($M_* > \langle M_{\rm GC} \rangle$). These nascent GCs are then assigned ages and metallicities corresponding to the age and metallicity of the burst in which they were formed. Each burst of star formation is assumed to be instantaneous, and each burst assumes instantaneous recycling of stellar material. Therefore, the metallicity distributions of the red GCs form a series of δ-functions, separated by the time elapsed between each burst.[†]

We then convert the ages and metallicities of each GC into observable quantities. The absolute metallicity, Z, predicted by GALFORM is converted to the amount of metals relative to hydrogen via $[{\rm m/H}] = \log(Z/Z_\odot)$, assuming $Z_\odot = 0.019$ (Anders & Grevesse 1989). In the observational plane, metallicity is often expressed as the ratio of iron-peak elements relative to hydrogen, [Fe/H], and Galactic halo stars and GCs are known to be α-enhanced with respect to solar values by $\sim +0.3$ (Carney & Harris 2001). Therefore, where appropriate, we convert between [m/H] and [Fe/H] using the approximate relation $[{\rm Fe/H}] = [{\rm m/H}] - 0.3$.

Broad-band colours, such as $V - I$ and $V - K$, are then derived for the GCs using the predicted ages and metallicities of our model. For this purpose, we use the single stellar population (SSP) models of Kurth, Fritze-v. Alvensleben, & Fricke (1999; henceforth KFF99). We have investigated the effects of using the KFF99 models which adopt both Salpeter and Scalo initial mass functions (IMFs). We find altering the assumed IMF has little effect on the *overall* colour distributions of the GC systems, and for the remainder of this study we use the KFF99 models which employ a Salpeter IMF.

2.2.2 Selecting the Initial Parameters

The principal parameters which we adjust are the formation efficiencies of the red and blue GCs. Several workers have argued for a 'universal' efficiency of GC formation (e.g. di Fazio & Capuzzo Dolcetta 1987; McLaughlin & Pudritz 1996; McLaughlin 1999), whilst other studies indicate that the star and GC formation efficiency in star-bursts and interactions may be significantly higher than in the 'passive' mode (e.g. Meurer et al. 1995; Zepf et al. 1999; Larsen & Richtler 2000; Ashman & Zepf 2001). Since the exact physical processes governing GC formation are still unknown (e.g. Elmegreen & Efremov 1997), rather than adopting *a priori* assumptions in any one particular direction, we have elected to employ a straightforward parametrisation for the GC formation.

We have chosen to adjust the GC formation efficiencies in our model in order to reproduce the numbers of GCs observed in the prototypical bimodal GC system of NGC 4472, perhaps the best-studied elliptical galaxy in terms of its GC system. This galaxy, an E2/S0 in the Virgo cluster with $M_B = -22.05$, has some 4000 blue GCs and 2400 red GCs (Geisler, Lee, & Kim 1996; Lee, Kim, & Geisler 1998), yielding a ratio of blue to red clusters of $N_{\rm blue}/N_{\rm red} = 1.6$.

[†] Our assumption of instantaneous GC formation is not strictly correct. Observational evidence (e.g. Whitmore et al. 1999) and theoretical work (Mihos & Hernquist 1996) on such induced star formation indicates that its duration may be of order ~ 100 Myr.
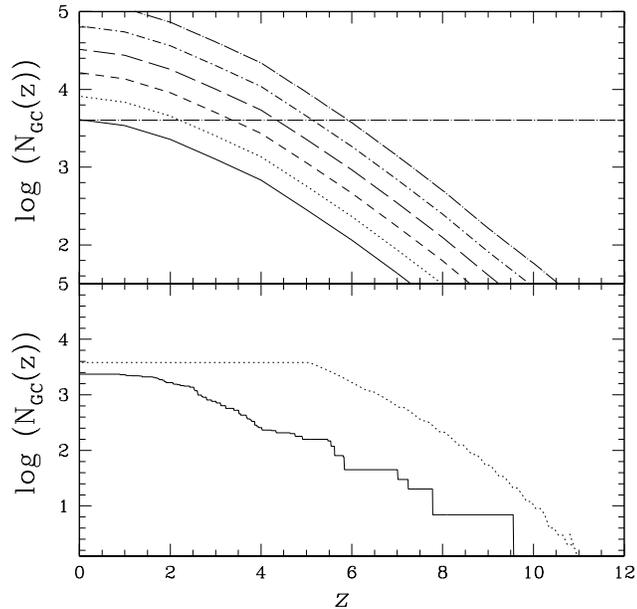
Figure 3. Cumulative number of GCs formed with redshift for our fiducial galaxy. *Top panel:* logarithm of the number of blue GCs formed in our fiducial galaxy with redshift. The different curves (left to right) indicate GC formation efficiencies of 0.00012 to 0.0040. The horizontal dot-dashed line indicates the observed number of blue GCs in NGC 4472. *Bottom panel:* comparison of the number of blue GCs formed with redshift in PGDs (dotted line) and red GCs in bursts (solid line), normalised to the observed numbers of red and blue GCs in NGC 4472 at $z = 0$. The efficiencies are $\epsilon_{\rm blue} = 0.002$ and $\epsilon_{\rm red} = 0.007$, and the blue GC formation has been truncated at $z = 5$.

Figure 4. The resulting metallicity distributions (left panels) and corresponding $V - I$ colour predictions (right panels) for the red and blue GCs in our fiducial galaxy under different assumptions. The distribution in [m/H] of red and blue GCs if *(a)* blue GC formation is allowed to continue to $z = 0$, with the efficiency of the blue GC formation assumed to be constant at $\epsilon_{\rm blue} = 0.00012$. *(b)* blue GC formation continues to the present epoch, but with $\epsilon_{\rm blue} \propto$ SFR and *(c)* $\epsilon_{\rm blue} = 0.002$, but blue GC formation is truncated at $z = 5$. The ages and metallicities are converted to colours using the models of KFF99.

We have selected an elliptical in our simulated sample (see § 2.2.3) which offers the closest match to NGC 4472 in terms of luminosity, morphology and halo mass.

The galaxy in question, #12 in our model sample, is a giant elliptical with $M_B - 5 \log h = -22.04$, and a dark matter halo rotational velocity ($V_{\rm rot}$) of 600 kms^{-1}. Assuming an isothermal potential and isotropic velocity dispersion, we convert $V_{\rm rot}$ to 1-D velocity dispersions, $\sigma_{\rm 1D} = v_c/\sqrt{2}$ (Baugh, Cole, & Frenk 1996). This yields $\sigma_{\rm 1D} = 424$ kms^{-1}, slightly higher, but comparable to that of the NGC 4472 subcluster in Virgo, where $\sigma_{\rm 1D} = 390$ kms^{-1}(Binggeli, Tammann, & Sandage 1987). Henceforth, we will refer to this model elliptical as our fiducial galaxy.

In GALFORM, the (globally averaged) luminous star formation rate (SFR) reaches a maximum of $\sim 0.1\ h$ M$_\odot$ yr^{-1} Mpc^{-3} at redshift ~ 3, and is still approximately 15% of this value at the present epoch. If we adopt a common efficiency for both GC components, and allow blue GC formation to continue up to $z = 0$ in un-merged PGDs, the blue GCs dominate (by mass) over the red GCs by up to two orders of magnitude (depending upon the merger history of the parent galaxy).

To illustrate this effect, in Figure 3 (top panel) we plot the number of blue GCs formed with redshift for our fiducial galaxy, for a range of GC formation efficiencies of 0.00012 to 0.004. For comparison, we also show in the figure the number of GCs in the blue mode of the NGC 4472 GC sys-
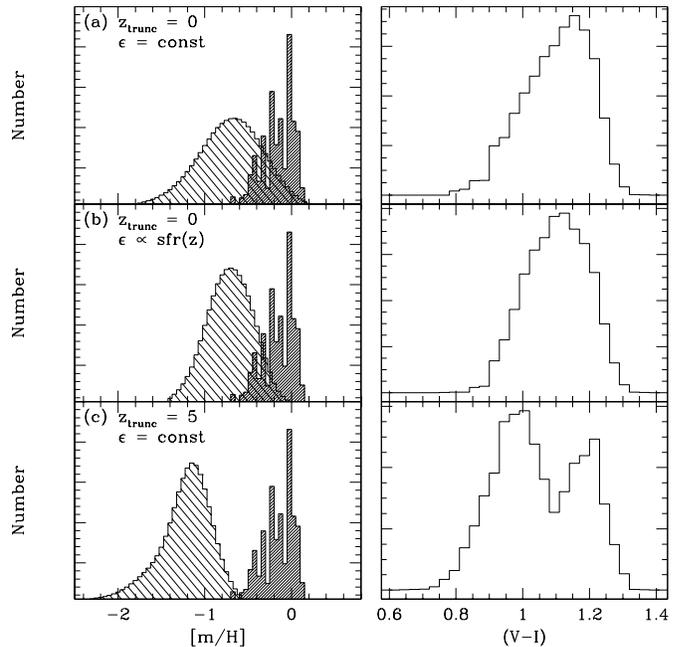
tem (~ 4000), taken from Geisler, Lee, & Kim (1996) (dot-dashed line). It is clear that, unless we assume a very low efficiency for GC formation, the PGD GC formation must be truncated at successively higher redshifts to obtain the correct total number of blue GCs. In the bottom panel of Figure 3, we show the cumulative total of blue GCs and red GCs formed with redshift. We have adopted efficiencies of $\epsilon_{\rm blue} = 0.002$ and $\epsilon_{\rm red} = 0.007$ to agree with the observed numbers of blue and red GCs in NGC 4472. The flattening of the curve for the blue GCs in Figure 3 indicates the location of our truncation redshift.

Upon initial consideration, it seems undesirable to arbitrarily truncate the formation of the blue GCs; we could simply choose a very low efficiency (e.g. $\epsilon_{\rm blue} = 0.00012$). However, by allowing blue GC formation to continue to the present epoch significantly broadens the blue GC metallicity distribution, to the extent that the observed colour distributions do not appear bimodal. Such a result is inconsistent with the present observational situation, not only for NGC 4472, but also for nearly all early-type galaxies with high-quality datasets.

In Figure 4 we show the differential metallicity distributions (left-hand panels) for the red and blue GCs formed in our fiducial galaxy. In producing the metallicity distributions of the red GCs (dark shaded histograms in left-hand panels), we assume a constant formation efficiency of $\epsilon_{\rm red}$

= 0.007. For the blue GCs we make three different assumptions about the nature of their formation efficiencies and formation redshift, each time ensuring that ~ 4000 GCs are created. In the right-hand panels, we show the corresponding $V - I$ colour distributions of the GCs, predicted by interpolating the KFF99 models for their corresponding metallicities and ages.

In Figure 4(a), we assume that blue GCs form in PGDs up until the present epoch, and adopt an efficiency of ϵ_{blue} = 0.00012, yielding ~ 4000 GCs in the blue mode. The blue metallicity distribution covers the range $-1.8 \leq$ [m/H] ≤ 0.2, peaking at [m/H] ~ -0.7, and overlaps substantially with the red GCs, which peak just short of solar metallicity. The peak-to-peak separation is ~ 0.5 dex and it is this, coupled with the fact that the distribution is so broad (~ 0.5 dex), which yields a colour distribution which is single-peaked and skewed to $V - I \sim 1.18$.

In (b) we again allow blue GC formation to continue to the present day, however this time we set ϵ_{blue} to be proportional to the SFR in their progenitor PGDs. We have based this assumption on the results of Larsen & Richtler (2000), who have performed observations of YMCs in 21 nearby spiral galaxies. These authors found that the specific U-band luminosity of YMCs is correlated with the host galaxy far-infrared luminosity. This, they propose, is indicative of the formation efficiency of the clusters being dependant upon the local SFR in the disc, as opposed to any dependence upon the *type* of star formation (e.g. merger, quiescent, starburst). By adopting $\epsilon \propto$ SFR, we find that the blue GC metallicity distribution becomes more sharply peaked than is the case for (a) and is narrower, with $\sigma_{rms} = 0.28$ dex. However, the mean of this distribution still occurs at [m/H] ~ -0.7. Likewise, the corresponding $V - I$ colours of the GCs also show a narrower distribution ($\sigma_{rms} = 0.22$ mag), but remain unimodal. At the peak of the SFR in the semi-analytic model ($z \sim 3$), mean stellar metallicities are already substantially enriched, therefore, in the present scheme, an $\epsilon \propto$ SFR relation yields blue GCs which cover too broad a metallicity range, and are too metal-rich (if no blue GC truncation is adopted).

In (c) we show the GC system formed in the same galaxy if we adopt a constant GC formation efficiency (ϵ_{blue} = 0.002), but truncate the blue GC formation at $z \sim 5$. This redshift corresponds to a characteristic mean gas surface-density of the progenitor disks of $\sim 1000 M_{\odot}$ pc^{-2} (1.25 $\times 10^{23}$ cm^{-2}). Such a truncation results in a blue GC distribution in the range $-2.4 \leq$ [m/H] ≤ -0.6, peaking at [m/H] ~ -1.2. Since the metallicity of the red GC component peaks at [m/H] ~ -0.2, this yields a peak-to-peak separation of 1.0 dex, and a corresponding colour distribution which is bimodal, with peaks at $V - I = 0.95$ and 1.18.

From the constraints placed upon us by observations of the GC system of NGC 4472, we obtain $\epsilon_{blue} = 0.002$ and $\epsilon_{red} = 0.007$ respectively. Furthermore, we truncate the formation of the blue GCs at $z = 5$ (henceforth denoted z_{trunc}), which corresponds to look-back times of ~ 12.3 Gyr in our assumed cosmology. We find that ϵ_{blue} is similar to the global value found by McLaughlin (1999) of $\epsilon = 0.0026 \pm 0.0005$, whilst ϵ_{red}, the GC formation efficiency in mergers, is required to be a factor of ~ 4 higher to produce the correct number of GCs.

We list the principal cosmological and model parameters adopted in this study in Table 1. In Table 1, f_{ellip} refers to the fraction of satellite to central galaxy mass required to induce a major merger (here, 30%), y is the yield assumed in calculating the metal-enrichment during star formation in PGDs and R is the fraction of mass recycled by stars. Again we refer the reader to Cole et al. (2000) for a full description of the model, and the effects of varying one or more of these parameters.

Table 1. Model parameters adopted in this study.

Adopted Cosmology	
Ω_0	0.3
Ω_b	0.02
Λ_0	0.7
h	0.7
Γ	0.19
σ_8	0.93
Mergers	
f_{ellip}	0.3
Star and GC Formation	
IMF	Salpeter
R	0.336
y	0.02
$\langle M_{GC} \rangle$	3.0×10^5 M$_{\odot}$
ϵ_{blue}	0.002
ϵ_{red}	0.007
z_{trunc}	5

2.2.3 The Galaxy Sample

We have simulated a total of 450 dark matter haloes, with masses $1.0 \times 10^{13} h^{-1} M_{\odot} - 1.3 \times 10^{15} h^{-1} M_{\odot}$. The associated 450 central galaxies (and their respective GC systems) span a magnitude range of $-23.6 \leq M_V$ - 5 log $h \leq -20.0$. The most luminous galaxies are rather rare constructs in GALFORM (as they are in the Universe), and therefore the lowest luminosity galaxies are numerically by far the most dominant in our simulated sample.

Our galaxies have bulge-to-total (B/T) luminosity ratios of 0.6 – 1.0. These B/T values roughly correspond to early-type galaxy morphologies (see Kauffmann, White, & Guiderdoni 1993; Baugh, Cole, & Frenk 1996). For convenience, in this paper we refer to low-luminosity ellipticals as those galaxies with $M_V - 5$ log $h \geq -21.5$, and define the division between field/group and cluster environments to lie (somewhat arbitrarily) at $\sigma_{1D} = 300$ kms^{-1} (i.e. velocity dispersions similar to that of the Leo group).

We emphasise the term 'environment' as used here refers to the velocity dispersion (mass) of the parent dark matter halo, rather than any number density measurement of nearby galaxies. Consequently, our definitions of field/group/cluster environments are not directly comparable to the density (ρ) parameter used by some previous workers.
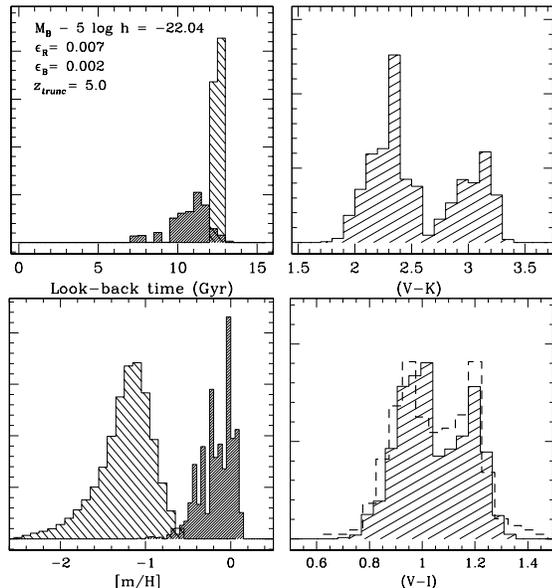
Figure 5. Age, metallicity and colour distributions for the GC system of our fiducial luminous elliptical galaxy. *Top left panel:* Age (look-back time) distributions for blue GCs (light shaded histogram) and red GCs (dark shaded histogram). *Bottom left panel:* Metallicity distributions for blue and red GCs. *Top right:* Predicted $V - K$ colours of GCs converted using the stellar population models of KFF99. *Bottom right:* $V - I$ colours of GCs using the KFF99 models. The uncertainty assigned to the colours is 0.05 mag. The dashed line indicates the scaled *HST* data for NGC 4472 from Larsen et al. (2001).

3 THE GLOBULAR CLUSTER SYSTEMS OF INDIVIDUAL GALAXIES

3.1 A Luminous Elliptical

In Figure 5 we show the age, metallicity and corresponding colour ($V - I$ and $V - K$) distributions obtained for our fiducial galaxy, the cluster elliptical with $M_B - 5 \log h = -22.04$. Inspection of the age histograms (top left, Figure 5) indicates that the mean age of the blue GCs is several Gyr older than the red GCs (although there is some small overlap), and possess a significantly shorter period of formation. This short duration of blue GC formation is a result of our truncation at $z = 5$, and the subsequent non-linear conversion between look-back time and redshift. The more extended and continuous formation of the red GCs is a consequence of ongoing merging and star formation from high redshift to $z \sim 0.6$.

The bottom left panel of Figure 5 shows the metallicity distribution of these same GCs. The blue GCs show an exponential-like increase in metallicity peaking at $[m/H] \sim -1.2$ and then a sharp cut-off which, again, is a result of our truncation. The metallicity range of these blue GCs is $-2.7 \leq [m/H] \leq -0.5$. In contrast, the red GCs form in multiple bursts at, or around, solar metallicities (there are 75 mergers involving star formation for this particular galaxy). Their metallicities extend from $[m/H] \sim -1.0$ to $[m/H] \sim + 0.2$, with a mean metallicity of $[m/H] = -0.2$. There is

very little overlap between the metallicity distributions of the two components.

The width of the blue and red metallicity distributions are 0.33 and 0.20 dex respectively. The model red GC distribution is somewhat narrower than those found from ground-based imaging by Geisler, Lee, & Kim (1996) for NGC 4472, which are 0.35 and 0.36 dex for the blue and red modes respectively. However, these values may be overestimated if the conversion between colour and metallicity is non-linear (e.g. see Kissler-Patig et al. 1998). Our values are closer to those found for the metal-poor and metal-rich components of the Milky Way of 0.34 and 0.23 dex respectively (Ashman & Zepf 1998).

In the top right panel we show the 'observed' $V - K$ colours of our fiducial galaxy's GC system, assuming observational uncertainties of 0.05 mag. The distribution is clearly bimodal, with peaks at 2.35 and 3.10 mag, and illustrates the sensitivity of $V - K$ colours to metallicity. The bottom panel shows the colour histogram in the less sensitive, but most commonly used $V - I$ colours. Again the colour distribution is bimodal - but not so well delineated as the $V - K$ indices - with peaks at 0.95 and 1.18 mag.

In the bottom-left panel of Figure 5 we have plotted the observed $V - I$ colour distribution of NGC 4472 GCs of Larsen et al. (2001), taken from three *HST* pointings. These data have been scaled to the total numbers of GCs produced in our model. Comparing the model $V - I$ distributions with data of limited spatial extent (e.g. *HST*) is not ideal, since the relative number of red to blue GCs changes with radius (e.g. Geisler, Lee, & Kim 1996) whilst we model the entire GC system. However, bearing this in mind we find that for our simulated GC system, the widths of blue and red modes in $V - I$ are 0.08 and 0.07 mag respectively, similar to the NGC 4472 data of Larsen et al. (2001) which have widths of 0.08 and 0.09 mag for the blue and red modes respectively.

The relatively old ages of the model GCs and the broad, distinct metallicity distributions shown in Figure 5 imply that the observed colour distributions are primarily driven by metallicity differences, consistent with our discussion in § 1.

3.2 A Low-Luminosity Elliptical

In Figure 6 we show our results for another GC system, this time for a lower luminosity elliptical galaxy, which has $M_B - 5 \log h = -20.42$. The age and metallicity distributions of the blue GCs in this galaxy are very similar to those shown for the more luminous elliptical in Figure 5. The blue GCs span the range $-2.5 \leq [m/H] \leq -0.6$, with a mean of $[m/H] \sim -1.2$. Indeed, for the majority of our simulated galaxies, variations in the age and metallicity distributions of the blue GCs are rather small. The principal differences in the distributions of the blue GCs is in the range of their metallicities for galaxies of different luminosity. We find that the most luminous galaxies possess blue GCs which reach to both slightly higher, and in particular, lower metallicities than galaxies of lower mass.

The distribution of metallicity for the red GCs in the low-luminosity elliptical is discontinuous, showing intermittent bursts of star formation. Indeed, the galaxy in question in Figure 6 has undergone 12 major mergers, a factor of ~ 6 fewer than its more massive counterpart. However, despite
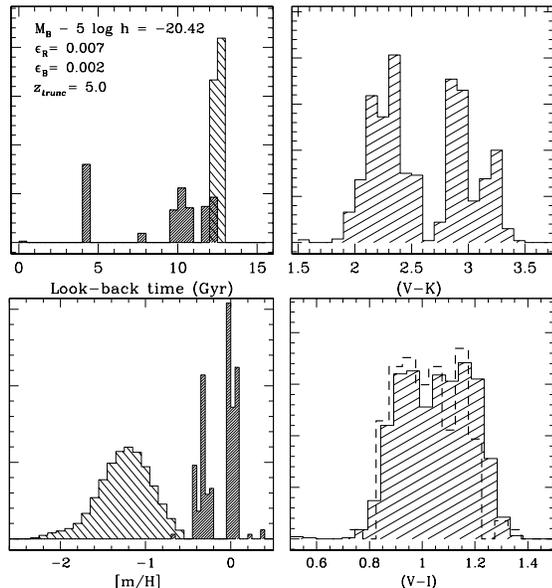
Figure 6. Age, metallicity and colour distributions for the GC system of a low-luminosity elliptical. *Top left panel:* Age distributions for blue GCs (light shaded histogram) and red GCs (dark shaded histogram). *Bottom left panel:* Metallicity distributions for blue and red GCs. *Top right:* $V - K$ colours of GCs using the SSP models of KFF99. *Bottom right:* $V - I$ colours of GCs derived from the KFF99 models. The dashed line indicates the scaled *HST* data for NGC 4552 from Larsen et al. (2001).

this much more modest merger history, the width and position of the red GC 'peak' is surprisingly similar to that of our fiducial galaxy. It is this trend, in that lower-luminosity ellipticals undergo fewer major mergers than more luminous galaxies, which is the origin of the scatter in the mean colours of the red GCs found in Section 4.2.

The age distribution for the red GCs in Figure 6 is somewhat different to that of our luminous fiducial galaxy. The distribution of the GC ages, corresponding to the look-back time of the galaxy's major mergers, extends to much younger ages. In fact, this galaxy has undergone a small merger coupled with GC formation recently (400 Myr ago) with a somewhat stronger merger occurring ~ 4 Gyr ago producing ~ 200 GCs (see next section) The existence of the very young GCs is reflected in the $V - I$ colours of the GCs shown in the bottom-right panel of Figure 6, which show a population with $V - I \sim 0.5$.

The ~ 4 Gyr ages of the 'red' GCs have the effect of slightly 'blueing' their $V - I$ colours, thereby yielding a broad, top-hat distribution as opposed to any obvious bimodality. However, this is actually a fairly rare occurrence in the model and only 1% of galaxies actually appear unimodal due to a spread in ages within the red GC sub-populations (see Sec 4.3). The $V - K$ colours (top-right panel) of the GCs again show their insensitivity to age differences for all but the very youngest clusters.

In general we find that, for lower luminosity galaxies, usually in lower circular velocity haloes, star formation in bursts occurs at successively later times. This reflects a generic result of semi-analytic models such as GALFORM,

in that more massive galaxies in cluster-type environments form their stars earlier than less massive galaxies in the field (we look more closely at this result in § 4.4).

In Figure 6, we have over-plotted *HST* data from Larsen et al. (2001) for NGC 4552, an E0 galaxy with $M_B = -20.47$, again scaled to the numbers in our model galaxy GC system. Whilst it is of similar luminosity to our model galaxy, we have primarily selected these galaxy data because its bimodality is *not* clearly delineated, providing reasonable agreement with our model GC $V - I$ colours. We emphasise that the majority of our simulated GC systems, for all galaxy luminosities, appear clearly bimodal in $V - I$, when the entire GC system is considered.

4   GLOBAL PROPERTIES OF THE GLOBULAR CLUSTER SYSTEMS

4.1   Specific Frequency

A commonly measured property of a galaxy's GC system is its total number of GCs. When normalised to the luminosity of a 'typical' dwarf galaxy ($M_V = -15$; Harris & van den Bergh 1981) this becomes the specific frequency:

$$S_N = N_{\rm GC} \times 10^{0.4(M_V + 15)} \qquad (2)$$

where $N_{\rm GC}$ is the total number of GCs associated with the galaxy in question with magnitude M_V. Since S_N relates the total number of GCs to the luminous mass of its parent galaxy, it is an indication of the efficiency of a given galaxy at forming GCs, and also offers an insight into the possible rôle of environment upon the properties of GC systems.

We show the luminosity growth and the corresponding evolution of S_N of our fiducial galaxy, and it low-luminosity counterpart in Figure 7. The fiducial elliptical shows a very smooth increase in its luminosity, with some 90% of its stellar component formed prior to $z \sim 1.0$ (a look-back time of ~ 8 Gyr in our assumed cosmology). Consequently, the evolution of the S_N in this galaxy's GC systems is also very smooth. The S_N of the blue GCs is initially very high at early times, and subsequently declines, taking on a constant value at $z \sim 0.4$. This occurs because the blue GCs are all created prior to $z = 5$, whereas the bulk of the galaxy stars form somewhat later. In contrast, the S_N of the red GCs in our fiducial galaxy show very little evolution. The creation of red GCs in mergers prior to $z \sim 0.4$, is effectively offset by the formation of field stars, thereby producing a near constant S_N. The observed decline in the *total* S_N at early times is entirely due to the contribution from the blue GCs.

The luminosity growth of the lower-luminosity elliptical is somewhat different. There is a sudden increase – a 'kink'– which occurs at ~ 4 Gyr, indicating that the luminous mass of the galaxy increases by $\sim 6\%$. This kink corresponds to a major merger which this galaxy undergoes, leading to the formation of field-stars and ~ 200 red GCs (see top-left panel of Figure 6). Significantly, this late merger has very little effect upon the total S_N of this elliptical. Since the formation of the red GCs during this merger is accompanied by the formation of some $2 \times 10^9 L_\odot$ of luminous material, the S_N of the red GCs increases by ~ 0.5 whilst the S_N of the blue GCs *decreases* by ~ 0.2. Therefore, the overall effect of this merger upon the total S_N of the galaxy is only to increase S_N
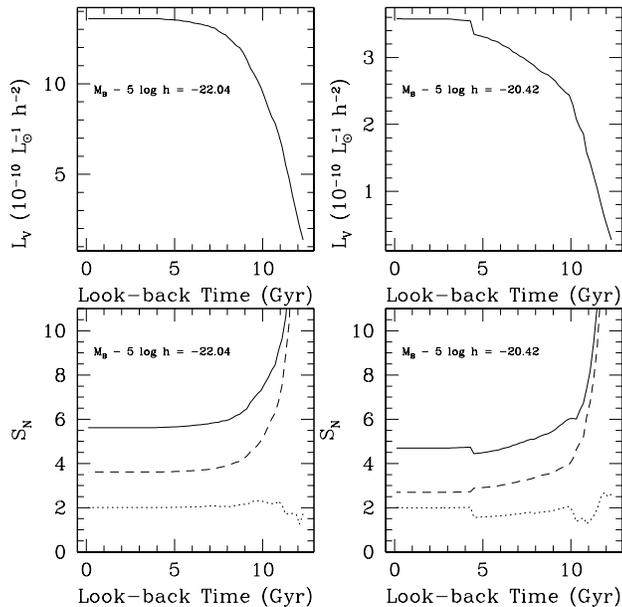
Figure 7. The evolution of specific frequency with look-back time for two model ellipticals. *Top left:* the luminosity growth of our fiducial galaxy. *Bottom left:* S_N of the red GCs (dotted line), blue GCs (dashed line) and total GC system (solid line). *Top right:* the luminosity growth of the elliptical with $M_B - 5 \log h = -20.42$. *Bottom right:* S_N of the red GCs (dotted line), blue GCs (dashed line) and total GC system (solid line). The 'kinks' in the two right-hand panels occurring at ~ 4 Gyr correspond to a major merger.

Figure 8. Dependence of S_N upon halo velocity dispersion. Small circles indicate the S_N of the model galaxies, the solid line indicates the mean value of this S_N. Data are taken from Ashman & Zepf (1997), Blakeslee et al. (1997) and Kissler-Patig (1997). Open circles represent brightest cluster galaxies (BCGs) and/or cD galaxies, filled triangles represent 'normal' ellipticals and open triangles indicate S0s.

by ~ 0.3. Therefore, we find that low-redshift mergers have no significant effect upon the S_N of ellipticals in our model, reflecting the relatively small cold gas fractions involved in mergers at these epochs.

In Figure 8 we show the total S_N of our elliptical galaxies plotted against the velocity dispersion of their dark matter haloes. Here, we use σ_{1D} as a measure of cluster mass, obtained from the halo circular velocity, V_{disc}, as discussed in § 2.2.2. It is important to realise that the luminosities of the central dominant galaxies in GALFORM (i.e. all the galaxies in this study) are strongly correlated with σ_{1D}. This is a natural result of semi-analytic galaxy formation models, where galaxies acquire mass through merging within dark matter haloes.

In Figure 8, we have also plotted data for 75 early-type galaxies, predominantly taken from the compilations of Kissler-Patig (1997) and Ashman & Zepf (1998). To increase the number of luminous galaxies in our observational sample, we have also included the data of Blakeslee (1997) and Blakeslee, Tonry, & Metzger (1997). These authors obtained S_N for 21 ellipticals in 19 Abell clusters (19 of which were brightest cluster galaxies, henceforth BCGs) using surface-brightness fluctuation techniques. Since Blakeslee, Tonry, & Metzger (1997) measured a 'metric' S_N, measured within a 40 kpc radius of each galaxy, we convert these to global S_N values, using the empirical conversion factor found by Harris, Harris, & McLaughlin (1998) of $S_N = 1.3 \times S_N^{40}$.

We assign velocity dispersions for the parent group or cluster for each galaxy in the Kissler-Patig (1997) and Ash-
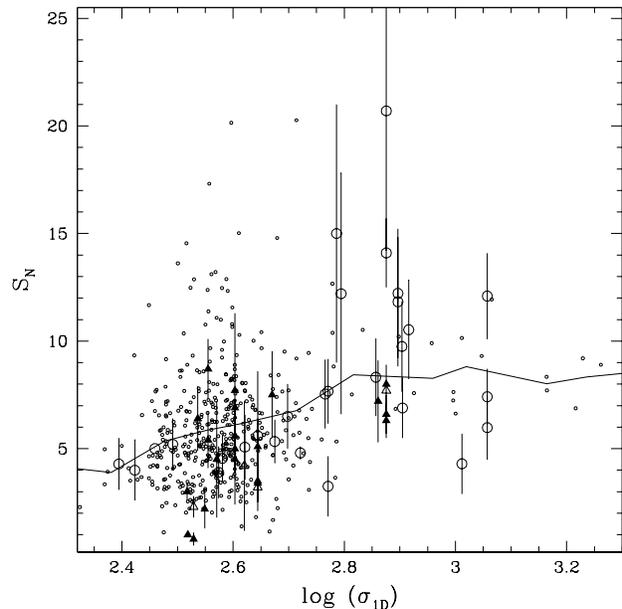
man & Zepf (1998) catalogues, based largely upon the galaxy group and cluster membership given in Rood & Dickel (1978). In the majority of cases, for groups we obtain velocity dispersions directly from NED. For the Blakeslee, Tonry, & Metzger (1997) sample, we use the velocity dispersions given in their paper (see Harris, Harris, & McLaughlin 1998 for a similar compilation).

Uncertainties in the total GC population of galaxies, which often require large extrapolations, lead to uncertainties in S_N of up to a factor of two for some galaxies (e.g. Ashman & Zepf 1998). This uncertainty is comparable to the scatter in S_N in the sample used here; therefore searching for variations in S_N for ellipticals at a given luminosity (e.g. Harris, Harris, & McLaughlin 1998) is difficult. However, the modelled GC systems shown in Figure 8 do reflect the observed scatter in S_N, but mainly amongst elliptical galaxies in haloes with $\sigma_{1D} < 630$ kms^{-1}.

For galaxies in the centres of clusters, S_N is known to correlate with the dynamical and X-ray mass of the host cluster (Blakeslee 1997; Blakeslee, Tonry, & Metzger 1997; Harris, Harris, & McLaughlin 1998). This behaviour is apparent in Figure 8, where many of the observed BCG/cD galaxies have S_N which are factors of 2–5 higher than their counterparts in lower velocity dispersion haloes. Interestingly, we find that the mean S_N of the model ellipticals also increases (by a factor of ~ 2) in going from the lowest to highest mass haloes, as indicated by the solid line in the figure. This is, initially, a rather surprising result. Since we have adopted *constant* GC formation efficiencies (as given in Table 1), one might expect S_N to remain approximately constant across all host galaxy magnitudes.

In order to explain the observed correlation between S_N and cluster mass, Blakeslee, Tonry, & Metzger (1997) posited that GCs formed at early times, and in proportion to the total mass available in the halo (including dark matter), whilst the luminosity growth of the central galaxy halted at later times, yielding the observed correlation of S_N with density. They interpreted the observed increase in S_N as a result of the fact that the BCGs were insufficiently luminous for their position in the cluster, i.e. the BCGs were under-efficient at forming field stars with respect to non-BCG galaxies, concluding that GCs formed with a constant rate per unit mass (0.7 GCs per $10^9 M_\odot$; $\epsilon \sim 0.0002$).

In a similar vein, Harris, Harris, & McLaughlin (1998), looked to the hot, X-ray emitting gas associated with galaxy clusters to explain the observed behaviour of S_N. By assuming a constant GC formation efficiency ($\epsilon \sim 0.001$), these authors argued that the baryonic material which would have gone on to form stars was expelled by galactic winds during star formation, effectively lowering the central galaxy's final *stellar* luminosity and effectively increasing its S_N.

Developing this idea, McLaughlin (1999) suggested that by considering the initial mass of gas available to the protogalaxy for forming stars on *similar spatial scales* to the galaxy starlight, the formation efficiency for GCs takes a constant value ($\epsilon = 0.0026 \pm 0.0005$). Moreover, he proposed that the ratio M_{GC}/M_{stars} does not provide a true measure of ϵ in the most massive galaxies (as implied by their larger than average S_N), and that the seemingly greater efficiencies of BCGs in forming GCs stems from the fact that S_N only measures the mass contribution from *stars*, in addition to the fact that the $\mathcal{M}/\mathcal{L}$ ratios of elliptical galaxies vary systematically with their luminosity.

Since we explicitly know the hot gas fractions present in each galaxy's halo, we can explore these ideas within our model. We remind the reader that we have included no dynamical destruction of the GCs in our model, and therefore our definition of 'efficiency' (equation 1) should only be regarded as a true formation efficiency under this assumption.

McLaughlin (1999), defined the observed GC formation efficiency to include all the hot gas (M_{hot}) detected on the same spatial scale as the galaxy starlight:

$$\epsilon \equiv \frac{M_{GC}}{M_{stars} + M_{hot}} \equiv \frac{M_{GC}^{init}}{M_{gas}^{init}} \qquad (3)$$

where M_{GC}^{init} is the initial GC population (before any dynamical processes have acted upon the GCs) and M_{gas}^{init} the initial gas supply available to the protogalaxy. Under the assumption of a constant GC formation efficiency, McLaughlin (1999) found that the total number of GCs (N_{GC}), scaled thus:

$$N_{GC} \propto L_{V,gal}^{1.3} \left(\frac{M_{hot}}{M_{stars}} \right) \qquad (4)$$

where $L_{V,gal}$ is the V-band luminosity of the host galaxy. The scaling $L_{V,gal}^{1.3}$ comes from noting that the $\mathcal{M}/\mathcal{L}$ ratios of ellipticals systematically increase with their luminosity, a result similar to those found previously by Djorgovski & Santiago (1992) and Zepf, Geisler, & Ashman (1994).

The scaling given in equation (4), is indicated by the dashed line in Figure 9. Here we have plotted the total number of GCs formed for each model galaxy, against host galaxy V-band luminosity (see figure 8 of McLaughlin 1999
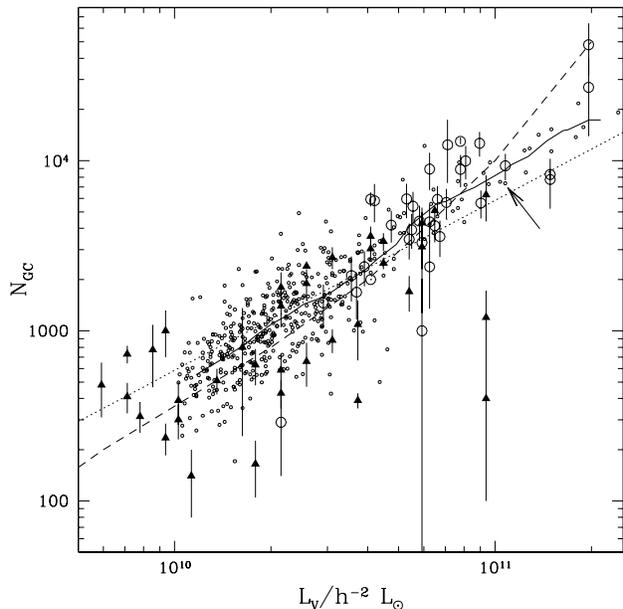

Figure 9. The total number of GCs formed compared to the luminosity of each galaxy. Small circles indicate the simulated GC systems of 450 galaxies. The dotted line indicates $S_N = 5$ (i.e. $N_{GC} \propto L^{1.0}$). The dashed line is the relation found by McLaughlin (1999), described in the text. The solid line indicates the mean value of N_{GC} for our model elliptical galaxies, the arrow indicates the position of our fiducial model galaxy. Data are taken from Ashman & Zepf (1997), Blakeslee et al. (1997) and Kissler-Patig (1997). Open circles represent brightest cluster galaxies and/or cD galaxies, filled triangles represent 'normal' ellipticals and open triangles indicate S0s.
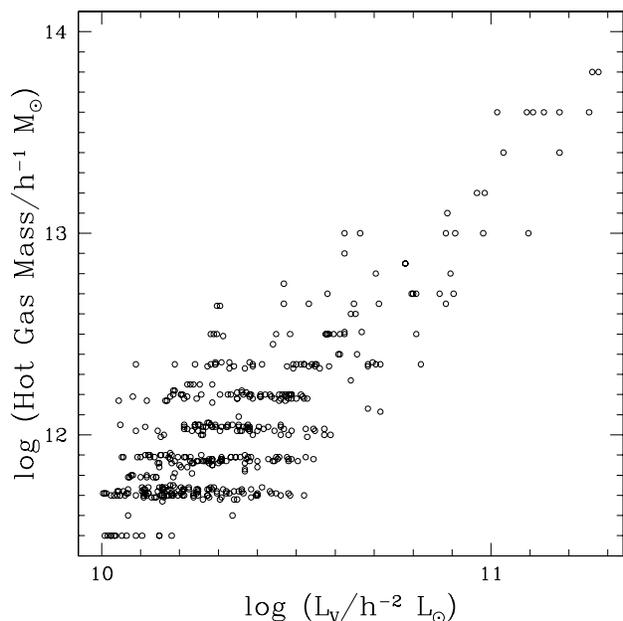

Figure 10. The total mass of hot gas associated with our model galaxy haloes.

for a similar plot). Again, we have included the observational data described previously.

The mean values of $N_{\rm GC}$ for the model ellipticals, systematically deviate from the $S_N = 5$ line (i.e. a scaling of $N_{\rm GC} \propto L_{V,\rm gal}^{1.0}$). Whilst the precise location of the model points in the y-axis depends upon our adopted efficiencies (the position of our fiducial galaxy is indicated in Figure 9), a least-squares fit to the model points indicates a scaling of $N_{\rm GC} \propto L_{V,\rm gal}^{1.25}$. The dependence of $N_{\rm GC}$ upon L for our model galaxies is similar to the scaling suggested by McLaughlin (1999; c.f. equation 4), to account for the observed increase in $\mathcal{M}/\mathcal{L}$ ratios of elliptical galaxies with luminosity. Since we have assumed $\epsilon = $ constant, and we have not included the model hot gas component in the calculation of $N_{\rm GC}$, the increase in model S_N can only be accounted for by an increasing $\mathcal{M}/\mathcal{L}$ ratio of our elliptical galaxies with increasing luminosity. As discussed by Benson et al. (2000; see their figure 8), the B-band $\mathcal{M}/\mathcal{L}$ ratios of galaxy haloes in GALFORM are a function of halo mass. For the halo mass range considered in this study $(1.0 \times 10^{13} h^{-1} {\rm M}_\odot \leq M_{\rm halo} \leq 1.3 \times 10^{15} h^{-1} {\rm M}_\odot)$, the $\mathcal{M}/\mathcal{L}$ ratio of galaxy haloes is an increasing function of L. This occurs because at $M_{\rm halo} > 10^{12} h^{-1} {\rm M}_\odot$, gas cooling is increasingly inefficient over the halo lifetime, thereby inhibiting galaxy formation (the most efficient value of $M_{\rm halo}$ is $\sim 10^{12} h^{-1} {\rm M}_\odot$, below these masses galaxy formation is inhibited by star formation feedback – see Benson et al. 2000).

The mean line of the model galaxies in Figure 9 scales in the correct sense with the observational data, and the McLaughlin (1999) relation. However, the model is still inconsistent with the highest S_N galaxies (although it may be argued that the scatter is large enough to be consistent). To account for this remaining discrepancy, McLaughlin (1999) included the hot gas component in the calculation of $N_{\rm GC}$, as indicated by equation 4.

We show the behaviour of the model hot gas component in Figure 10. Here, 'hot gas' refers to all the baryonic material in the halo which is not in the form of cold gas or stars. Figure 10 indicates that the most massive central cluster galaxies are able to expel and virialize large quantities of gas at early times, due to a combination of feedback from star formation, and long gas-cooling time-scales. This picture is supported by the observational studies of Harris, Harris, & McLaughlin (1998) and McLaughlin (1999). Moreover, it is also clear that the halo hot gas component of our model ellipticals increases much *too* strongly (by a factor of ~ 100) to account for the differences shown in Figure 9.

However, consideration of this apparent inconsistency with the McLaughlin (1999) study must be accompanied with an important caveat. The X-ray gas considered by McLaughlin was measured on < 100 kpc scales (i.e. on scales where the galaxian surface brightness can be measured), whereas the hot gas component in GALFORM is associated with the entire galaxy halo (i.e. on ~ 500 kpc scales). Associating some core radius of hot gas in our model with galaxy luminosity is not particularly meaningful, since in our model the entire hot gas component is associated with the star formation in the central galaxy. Our scheme is more in keeping with the interpretations of West et al. (1995), Blakeslee, Tonry, & Metzger (1997) and Harris, Harris, & McLaughlin (1998), in that the 'high S_N' problem is associated with entire haloes (e.g. clusters), rather than on the more local
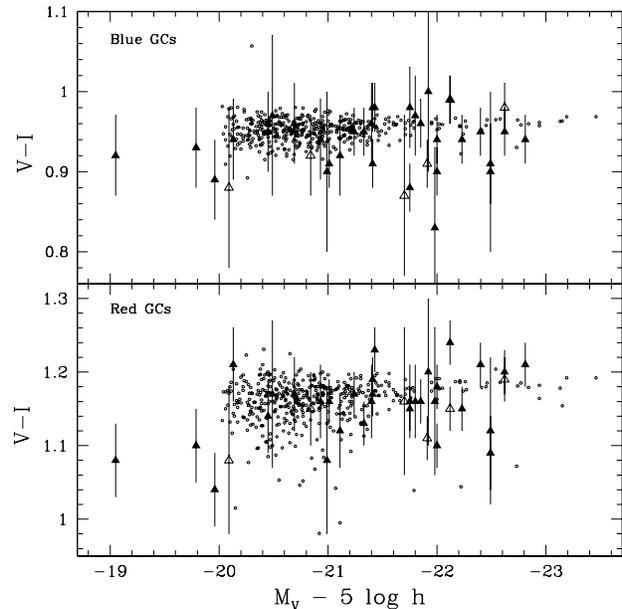

Figure 11. The mean colours of the GC systems with host galaxy magnitude. *Top panel:* blue GCs, *bottom panel:* red GCs. Data points with error-bars taken from the compilation of Forbes & Forte (2001). Open triangles represent the GC systems of S0 galaxies, filled triangles represent galaxy types earlier than S0,

scales as suggested by McLaughlin (1999). These interesting issues will be examined in greater detail in a future paper.

4.2 Mean Colours

Since the initial study by van den Bergh (1975), the subject of whether or not the mean metallicities of GC systems (and their sub-populations) correlate with host galaxy luminosity has been a controversial one (e.g. Brodie & Huchra 1990; Ashman & Bird 1993; Secker et al. 1995; Durrell et al. 1996; Forbes et al. 1996; Kundu & Whitmore 2001; Forbes & Forte 2001; Larsen et al. 2001). Since in our model, we have information about the stellar populations of both the GCs and their host galaxies, we are in a position to look for any such correlations between these two properties.

In Figure 11 we have plotted the mean $V - I$ colours of the red and blue GCs predicted by our model against the absolute V-band magnitude of the host galaxy. The datapoints are taken from the compilation of Forbes & Forte (2001), who have placed the GC colour distributions of 28 galaxies onto a common $V - I$ system. To facilitate a fair comparison, we have omitted all the galaxies from the Forbes & Forte (2001) compilation with morphological type later than S0.

For both the red and the blue GCs, our model points lie comfortably within the observational uncertainties of these data. The large scatter in our model at the low-luminosity end arises partly because of the occurrence of late bursts of GC formation, where age effects become important in determining the colours of the GCs.

Our model predicts an essentially flat relation between host galaxy magnitude and mean (although there is an in-

crease in both sub-populations at the 1-σ level). Forbes & Forte (2001) found that the mean $V - I$ colours of the red GCs increased with both host galaxy luminosity and velocity dispersion. These authors argued that such a correlation was indicative of a close connection between the red GCs and the bulk stellar content of their host galaxy, and that this connection primarily supported the multi-phase collapse model of Forbes, Brodie, & Grillmair (1997). Interestingly, Kundu & Whitmore (2001) also found evidence for such a correlation (from the thesis work of A. Kundu, from which part of the Forbes & Forte sample was derived), however these authors did not ascribe any particular significance to their findings, and argued that such a correlation did not support any one particular GC formation model.

At face value, the flat colour-magnitude gradients of the model GC systems indicate that either *(i)* the GCs do not 'know' about their host galaxy, implying that the GCs do not share a common chemical enrichment history with the galaxy or *(ii)* all the galaxies in our sample are enriched to very similar levels.

We know the former scenario not to be the case, since in our scheme the formation of red GCs is tied to the star formation which is associated with major mergers. Any subsequent increase in the metallicity of these bursts would lead to enrichment of the GCs, and therefore be reflected in their colours. The situation for the blue GCs is not so clear, since we truncate their formation at the early stages of the formation of their host galaxy. However, it seems reasonable to expect that enrichment in these GCs will have preceeded to similar levels irrespective of the final mass of the galaxy, leaving little or no correlation between their mean colours and host galaxy luminosity.

To better understand these results, we look at the behaviour of the GC mean colours their parent galaxies with galaxy magnitude in Figure 12. The mean colours of the galaxy sample are determined from the mass-weighted age and metallicity of their stellar populations, however we find that by adopting a luminosity-weighting scheme has little effect on the colours. We have not included any corrections for aperture in the colours of the galaxies, which can have a significant effect on their mean colours (e.g. Kodama et al. 1998). However, since we have no spatial information about the stellar populations in our sample and we cannot correct for the presence of radial gradients which are seen in real galaxies, we simply state that the galaxy colours given in Figure 12 are a lower limit.

The figure shows that the mean colours of the red GCs are generally consistent with the mean galaxy colours, although for the most luminous galaxies the GC colours are marginally *redder* than the galaxies. The blue GCs are some 0.2 mag bluer in $V - I$ than their host galaxy, corresponding to a pure metallicity difference of ~ 1.0 dex. This is consistent with all studies to date for which photometry of both the GC sub-populations *and* the host galaxy light have been obtained in the same observation (NGC 1399 : Ostrov, Forte, & Geisler 1998, NGC 1427 : Forte et al. 2001, NGC 3923 : Zepf, Ashman, & Geisler 1995, NGC 4472 : Geisler, Lee, & Kim 1996; Lee & Kim 2000), as noted by Forbes & Forte (2001).

Figure 12 also highlights another important issue: the mean model galaxy colours show no increase with magnitude. Indeed they exhibit very similar behaviour to that of
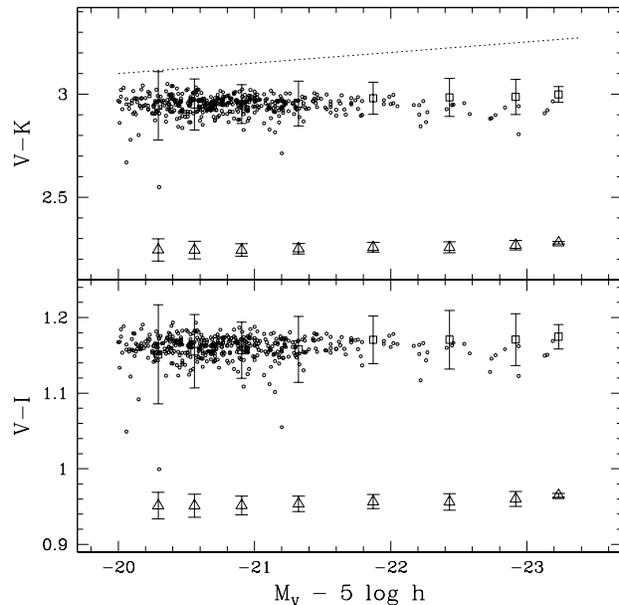

Figure 12. The mean colours of the GCs and their host galaxies, versus parent galaxy magnitude. *Top panel:* Mean $V - K$ colours of the red GCs (squares with 1σ error-bars), blue GCs (triangles with 1σ error-bars) and model galaxies (small circles) versus galaxy M_V. The dotted line indicates the slope of the galaxy colour-magnitude relation for Coma galaxies from Bower et al. (1992). *Bottom panel:* Same for $V - I$ colours.

the GCs. Compare this to the colour-magnitude (C-M) relation found for Coma cluster galaxies by Bower, Lucey, & Ellis (1992), indicated by the dotted line in the top panel of Figure 12. The lack of a significant colour gradient amongst the red GCs is seemingly a manifestation of the inability of the semi-analytic models (including GALFORM) to naturally reproduce the observed C-M relation of galaxies. Whilst at the lowest luminosities ($M_V - 5 \log h \geq -19.0$), the slope of the C-M relation is recovered (e.g. see figures 10 & 13 of Cole et al. 2000), above this the mean galaxian metallicities reach a peak beyond which chemical enrichment does not proceed further. This precludes any increase in the mean galaxy colour, thereby giving rise to a flat (or even negatively sloped) C-M relation.

Such behaviour can be remedied by assuming extremely strong feedback, as was shown by Kauffmann & Charlot (1998). However, adopting very large values for the feedback efficiency yields unphysical results in other predictions of GALFORM (see Cole et al. 2000 for details). This failure of the semi-analytic models probably belies our lack of understanding of the complex processes of star formation, and is beyond the scope of this paper.

4.3   Bimodality

One of the motivations of this study is to reproduce the observed bimodality of GC systems, and in doing so attempt to understand their physical origins. In § 2.2.2, we found that it was necessary to truncate the blue GC formation
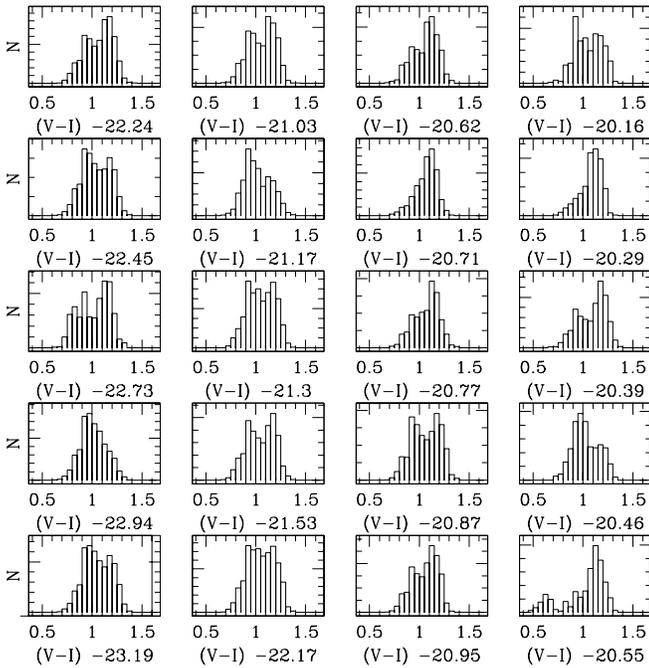
Figure 13. The $V - I$ colour distributions for a selection of simulated GC systems. The values at the bottom of each plot indicate the V-band magnitude ($M_V - 5 \log h$) of each galaxy. The distributions show a wide variety of morphologies, from principally blue-peaked, to bimodal, to strongly red-peaked.

Figure 14. The DIP statistic and mean colours of our model GC systems. *Top left:* DIP statistic for our simulated *HST* observations (solid lines), compared to the data of Gebhardt & Kissler-Patig (1999; dotted lines). *Top right:* Distribution of the DIP statistic for the complete model GC systems of each elliptical. *Bottom right:* mean $V - I$ colours of the complete model GC systems and *bottom left:* mean $V - I$ colours of our simulated *HST* observations (solid lines), compared to the data of Gebhardt & Kissler-Patig (1999; dotted lines).

at early times (i.e. $z = 5$) in order to reproduce GC colour distributions similar to those which are observed.

In spite of this enforced truncation of the blue GCs, the colour distributions of the entire GC systems show an appreciable variation in their morphologies. We show a selection of $V - I$ colour distributions for our simulated GC systems in Figure 13. The galaxy GC systems are ordered by descending host galaxy magnitude (from the bottom left to top right in the figure). The colour distributions range from bimodal (e.g. the elliptical with $M_V - 5 \log h = -23.19$), to predominantly blue-peaked (e.g. $M_V - 5 \log h = -22.94$) and predominantly red-peaked (e.g. $M_V - 5 \log h = -20.29$). The elliptical with $M_V - 5 \log h = -20.55$ shows a number of GCs with $0.5 \leq V - I \leq 0.8$. This is the result of several recent mergers between this galaxy and satellites, which gives rise to significant star formation accompanied by GC formation.

In order to make a fair comparison between the GC colour distributions predicted by our model, and those observed, we must restrict our analysis of bimodality to some sub-sample of the GC population. Taking the study of Gebhardt & Kissler-Patig (1999) as being representative of a 'typical' *HST* observation of a GC system, we return to our bimodal prototype galaxy NGC 4472. From two *HST* pointings, these authors identified 486 GCs out of a total population of ~ 6400 GCs (Geisler, Lee, & Kim 1996), thus sampling approximately 8% of the total GC population of this galaxy. Whilst subsequent studies have gone deeper for this galaxy, and/or have increased pointings (e.g. Puzia et al.
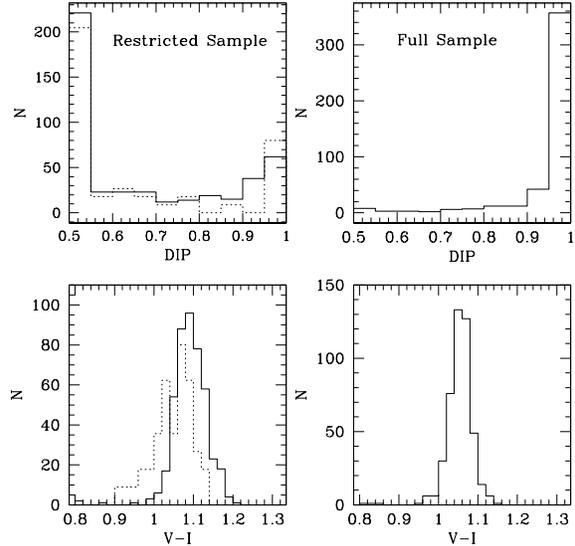
1999; Lee & Kim 2000; Larsen et al. 2001), we take the data of Gebhardt & Kissler-Patig (1999) as a lower limit.

To simulate these observations, we take a random distribution of GCs corresponding $\sim 8\%$ of each GC system. We then assign each of these GCs a luminosity, drawn randomly from an observed luminosity function. Specifically, the luminosity function adopted is that of NGC 4472, taken from Puzia et al. (1999). Finally, we assign photometric errors to each GCs colour (see Appendix A in Carney & Harris 2001):

$$\sigma_{\mathrm{phot}} \simeq 2.5 \times \log \left(1 + \frac{1}{(S/N)} \right) \tag{5}$$

where S/N is the signal-to-noise and σ_{phot} the photometric uncertainty.

To look for the presence of multiple populations in restricted datasets, statistical tests such as the KMM test (Ashman, Bird, & Zepf 1994) and the 'DIP statistic' (e.g. Hartigan & Hartigan 1985; Gebhardt & Kissler-Patig 1999) are often employed. The success of such tests necessarily depend, among other things, upon the size of the dataset considered. To place our results on a more quantitative footing, we have measured the DIP statistic and mean colours of the colour distributions of our full GC sample and simulated *HST* observations. The DIP statistic is a non-parametric test whose null hypothesis is that a distribution is unimodal (see Gebhardt & Kissler-Patig 1999). A value near 0.5 indicates likely 'uni-modality', whereas 1.0 indicates the presence of multiple sub-populations (not nec-

essarily bimodality, although for our model this is assumed to be the case).

We show the results of these statistical measures in Figure 14. The left-hand panels in the figure show the results for our simulated *HST* observations, compared to the scaled data from Gebhardt & Kissler-Patig (1999). The right-hand panels in the indicate the results for our unrestricted model GC systems.

Figure 14 indicates that both the model *HST* observations and data are distributed in a similar manner, with a large 'spike' at 0.5 (uni-modality), and a somewhat smaller one at 1.0 (multi-modality), coupled with a relatively flat distribution of DIP values in between. The model predicts a slightly higher fraction of GC systems lying at DIP $0.8 \sim 0.9$ than is the case for the *HST* data. Gebhardt & Kissler-Patig (1999) separated their data into three groups, those galaxies which showed a clear deviation from uni-modality, those which had DIP values higher than 0.5 at greater than 1σ significance and galaxies which appeared to have unimodal GC systems. We have performed the same division on our data, using the same definitions as Gebhardt & Kissler-Patig (1999). We define 'certain' as systems which are deemed bimodal by the DIP statistic, 'likely' as likely bimodal, and 'unimodal' as those GC systems which do not appear bimodal.

From our 450 GC systems, we obtain a relative fraction (certain : likely : unimodal) of 86 : 118 : 246, or 19% : 26% : 55%. These values are similar to the Gebhardt & Kissler-Patig results, which comprise of 21% : 26% : 53%. However, we find that these values are extremely sensitive to the model 'photometric errors' which we adopt. Increasing the mean uncertainties by only 0.01 mag in $V-I$, yields a ratio of 16% : 25% : 59% (i.e. more bimodal systems are hidden by photometric errors), likewise, reducing the uncertainties by 0.01 mag results in a 24% : 30% : 45% split. This sensitivity to photometric errors is probably the origin of the different measures of bimodality for the same GC systems between different studies.

However, by obtaining the DIP statistic for our unrestricted GC systems (right-hand panels in Figure 14), we find that 93% are intrinsically bimodal in $V-I$. Of the remainder, 4% fall into the 'likely' category and 3% are not bimodal.[‡] The majority of these latter 32 galaxies have less than 20 GCs in their total GC system, and small-number statistics become the dominant factor in determining the presence of sub-populations in these systems. Five galaxies (1% of the total) have undergone recent mergers coupled with the formation of GCs, which conspire to superimpose the red and blue GC sub-populations upon each other, giving apparently unimodal distributions in $V-I$. When examined in $V-K$ colours, three of these systems appear bimodal (the other two are effectively present-day mergers, and therefore even the $V-K$ colours are extremely blue). Thus, in our model, the GC systems of nearly all large elliptical galaxies are intrinsically bimodal in broad-band colours, which

---

[‡] The DIP statistic is somewhat more conservative than some other statistical methods for detecting bimodality in datasets. Applying the homoscedastic (a common covariance) KMM test to our results indicates that 96% of the model GC systems are not unimodal at high confidence.
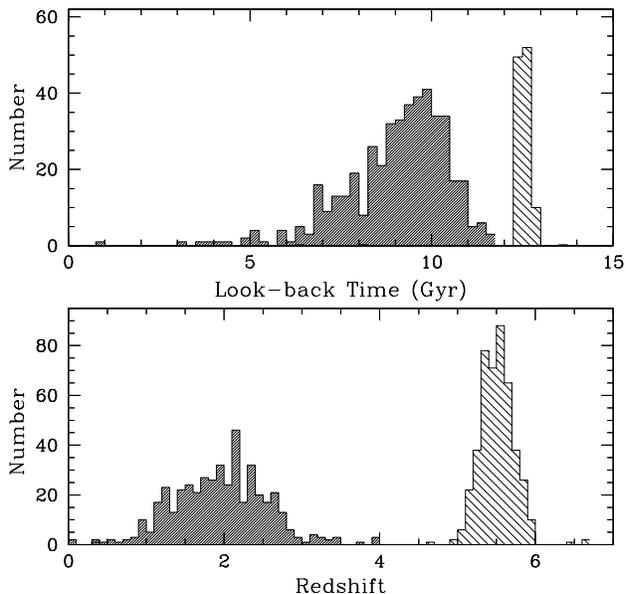

Figure 15. The distribution in mean ages for all 450 model GC systems. *Top panel:* Distribution in look-back time for the red GCs (dark shaded histogram) and blue GCs (light shaded histogram). The blue GC histogram has been scaled down by a factor of 6 for display purposes. *Bottom panel:* Distribution in formation redshift for the red and blue GCs.

is detectable if the total GC population can be 'observed'. It then follows that since nearly every non-detection of bimodality (from an intrinsically bimodal parent distribution) is attributable to photometric errors and/or small-number statistics, (irrespective of whether our model is correct or not), any conclusions relating to the colour distributions of GC systems obtained from observations of only limited depth and spatial extent should be made cautiously.

The bottom-left panel of Figure 14 compares the biweight estimate of the position (sample mean) of the $V-I$ peaks of the simulated *HST* observations and observational data. The position of the peaks are similar, with $V-I = 1.09$ and $V-I = 1.05$ for model and data respectively, whilst the distribution in the model colours is slightly narrower than that of these data, with $\sigma_{\rm rms} = 0.049$ and $\sigma_{\rm rms} = 0.052$ respectively (the *HST* data has been scaled by a factor of $\sim$ 9 in the figure). For the unrestricted model GC systems, the mean $V-I$ colours is 1.06, with a dispersion of 0.035 mag. The relatively narrow distribution of these colours indicates that the mean of the GC colour distributions is fairly insensitive to the varied merger histories of the individual galaxies.

4.4   Ages of the Globular Clusters

A key observational test of the various models for the formation of GC systems lies in determining their age. In our model, we know the formation redshift of each GC, and therefore we can look at the age distributions of GCs amongst our galaxy sample.

In Figure 15 we show the mean age (look-back time) and formation redshift distributions for our model GCs (the
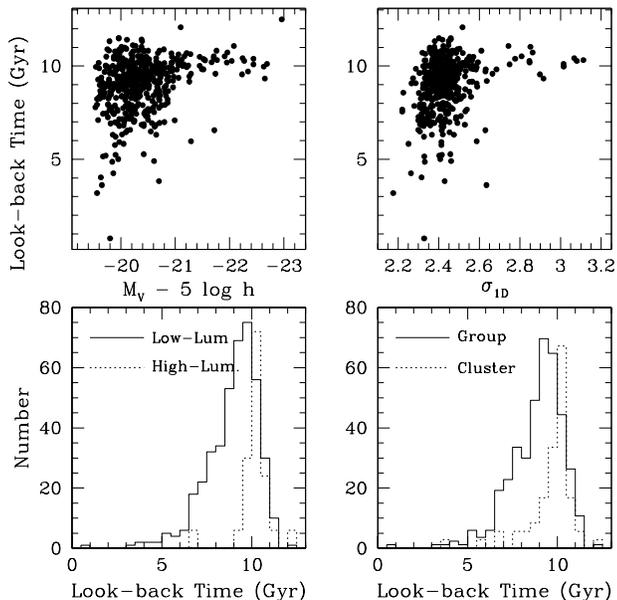
Figure 16. The mean ages of the red GCs as a function of host galaxy properties. *Top left panel:* Mean ages of the red GCs as a function of host galaxy absolute magnitude. *Bottom left panel:* Histogram of the mean GC ages, separated into high and low-luminosity ellipticals. The histogram for the high-luminosity galaxies has been scaled by a factor of 3 for display purposes. *Top right panel:* Mean ages of the red GCs as a function of halo velocity dispersion. *Bottom right panel:* Histogram of the mean red GC ages, separated into field/group and cluster environments. The histogram for the field/group galaxies has been scaled by a factor of 5 for display purposes.

cosmological parameters adopted are given in Table 1). Perhaps the most striking feature in the figure is the narrow range of mean ages occupied by the blue GCs, at ~ 12.3 Gyr (top panel). This mean age for the blue GCs is consistent with the 'favourite' age of Galactic GCs found by Carretta et al. (2000) of 12.9 ± 2.9 Gyr. Whilst the onset of blue GC formation begins as soon as enough gas cools to begin forming stars (at $z \sim 11$; c.f. Figure 3) the vast majority of blue GCs form at or around our truncation redshift.

The red GCs clearly form over a more extended period, with mean redshifts of formation from $z \sim 4$ to the present day. However, red GCs *begin* to form in small numbers at $z = 9 \sim 10$ during the onset of PGD merging (e.g Figure 3). The mean ages of the red GCs occurs at 9 Gyr ($z \sim 2$), although the skewed nature of the age distribution means that the peak of red GC formation actually occurs ~ 10 Gyr ago. This gap in the formation redshifts of the blue and red GCs is key to the metallicity differences between the GCs. The material fed-back to the interstellar medium after the first period of GC formation has time to cool and form GCs through merging at a later epoch.

The short duration of the blue GC formation makes comparisons of their ages with other galaxy properties difficult. Moreover, the mean ages of the blue GCs are clearly sensitive to the exact redshift of their truncation. However, this is not the case for the red GCs, which form over a significant fraction of a Hubble time. In Figure 16, we show the

mean ages of the red GCs as a function of their host galaxy magnitude and halo velocity dispersion. The behaviour of mean ages of the red GCs with host galaxy luminosity and halo velocity dispersion are very similar. The highest luminosity galaxies, and those galaxies in the highest σ_{1D} haloes both give rise to red GCs with ages ~ 10 Gyr, with small scatter. In proceeding to lower luminosities (and lower σ_{1D}), this scatter in mean age increases sharply, with a tendency for the GCs to possess younger ages.

In the bottom panels of the figure, we show histograms of the mean GC ages separated by their host galaxy properties, according to our definitions given in § 2.2.3. We find that the red GCs associated with low-luminosity ellipticals have mean ages of 8.8 Gyr ($\sigma_{\rm rms} = 1.4$ Gyr), whereas for the high-luminosity galaxies the mean age of the GC systems is 10.0 Gyr ($\sigma_{\rm rms} = 0.8$ Gyr). Similarly, the GC systems associated with ellipticals in the field and/or groups have mean ages of 7.9 Gyr ($\sigma_{\rm rms} = 1.7$ Gyr), whilst those in clusters have mean ages of 9.2 Gyr ($\sigma_{\rm rms} = 1.3$ Gyr). Clearly, these values will change depending upon the exact nature of the definitions of 'low-luminosity elliptical' or the field/group and cluster environments, however the general trends will remain.

5 DISCUSSION

There now seems little doubt that GCs are formed during the merging and interaction of galaxies which involve star formation (e.g. Schweizer 2001). In this regard a metal-rich GC component arises naturally in a hierarchical model such as GALFORM, which predicts many such mergers over a broad distribution of redshifts. However, to what *degree* these merger-formed GCs contribute to the red peak associated with the GC populations of elliptical galaxies is uncertain.

In our scheme, continuous gaseous merging produces the entire red GC sub-population observed in ellipticals, and the ages of these GCs directly reflect the redshifts at which their host galaxy underwent major mergers involving star formation. In this way, the red GCs represent a direct probe of the dynamical and stellar assembly of their host galaxies. As shown previously, the red GC sub-populations of our model ellipticals possess significant age structure in any given galaxy. Moreover, the scatter in this age structure is predicted to increase with decreasing host-galaxy luminosity and decreasing dark matter halo velocity dispersion, reflecting the occurrence of later star formation in these less-massive haloes. This is a principal result of this study, and provides a method of testing our simulations against other scenarios for forming the GC systems of luminous elliptical galaxies.

In the *in-situ* collapse model of Forbes, Brodie, & Grillmair (1997), two phases of galaxy collapse give rise to two GC populations enriched to significantly different levels. The first collapse produces metal-poor GCs with high efficiency with respect field stars, followed at some later time by a secondary collapse where the majority of the galaxy stars and metal-rich GCs are created. In common with our model, the metal-poor GCs are predicted to be several Gyr *older* than the red GCs, with the exact age difference depending upon the delay between the two collapses. If this delay

has a characteristic time-scale, such as that for the onset of type-I supernovae, then the age difference between the GC sub-populations is expected to be similar for galaxies irrespective of galaxy luminosity and halo velocity dispersion. Moreover, the metal-rich GCs are will be essentially *coeval*, since the time-scale for the secondary collapse is expected to be short.

Cote, Marzke, & West (1998) presented a model where the metal-poor GCs are captured from the surrounding galaxy population via tidal stripping and/or mergers, and the red GCs are somehow intrinsic to the host elliptical, in common with the *in-situ* model. These authors found that by adopting a relatively steep luminosity function of galaxies in the host galaxy cluster, the bimodality of GC metallicities could be reproduced without necessarily requiring two phases of star formation. Whilst Cote, Marzke, & West (1998) do not discuss in detail the possible mechanism for the formation of either GC sub-population, they do predict that there will exist *no* significant age differences between the GC sub-populations.

In many respects, the model presented here closely follows the original philosophy behind the Ashman & Zepf (1992) merger model. Merging creates metal-rich GCs, whilst the merger progenitors contribute their own population of metal-poor GCs to the final GC system. Since the spiral-spiral mergers of Ashman & Zepf (1992) are expected to occur at relatively high redshift, it may be argued that the distinction between the proto-galactic discs in our model and gaseous spirals in the Ashman & Zepf picture becomes ill defined.

However, although it might be tempting to associate these PGDs with the precursors of todays spiral galaxies, this is *not* the case. In the semi-analytic model as presented by Cole et al. (2000), spiral galaxies form through the accretion of cold gas onto bulges. Providing no further merging occurs, this gas will settle and remain in a stellar/gas disc. A large initial bulge mass with respect to the mass of accreted cold gas will correspond to an early-type spiral, and a less-massive bulge will correspond to a later-type spiral. An obvious extension of our model will be to study the GC systems of late-type galaxies, however the implication is clear: in our model, the bulges of spirals are formed in the same manner as those of ellipticals. Therefore, *the metal-rich GCs in spirals are associated with the bulge and/or thick disc, and the majority of spiral galaxies will have bimodal GC metallicity distributions.* This notion that the GCs of ellipticals and spirals have essentially the same origin finds observational support in the recent study of Forbes, Brodie, & Larsen (2001).

In our simulations, the progenitors of the blue GCs are exponential, proto-galactic discs, which at high redshifts, are largely gaseous. For example, at $z \sim 5$, these PGDs have mean cold gas-fractions of order 95%. We assume that these PGDs form, and continue to form, blue GCs (prior to our truncation redshift) unless they merge with the central galaxy in the dark matter halo. As suggested by Ashman & Bird (1993), it is then not difficult to imagine that any such PGDs which failed to merge are now represented by dwarf galaxies (e.g. the LMC), which have only managed to form metal-poor, blue GCs.

Observationally, perhaps the best candidates for such proto-galactic entities are damped Lyα systems (DLAs),

high-redshift H I systems with column densities $N_{H I} \geq 2 \times 10^{20}$ cm^{-2}, seen in absorption against background QSOs (e.g. Wolfe 1988). Burgarella, Kissler-Patig, & Buat (2001) have recently discussed the possible relation between metal-poor GCs and DLAs at high redshift. Prochaska & Wolfe (1997, 1998), have argued that the observed high velocity widths (~ 300 kms^{-1}) and asymmetry of DLA line-profiles are indicative of a population of rapidly rotating thick discs, which are incompatible with the slowly rotating exponential discs modelled in semi-analytic schemes (see Kauffmann 1996). However, Haehnelt, Steinmetz, & Rauch (1998) show that the same observations can be reproduced by modelling DLAs as gaseous systems which are supported by a mixture of random motions, merging, infall *and* rotation (see also Maller et al. 1999; Ma & Shu 2001). Such agglomerations, with virial velocities of ~ 100 kms^{-1}, are consistent with the PGD kinematics assumed in GALFORM.

In creating the metal-poor GCs, we found it necessary to truncate blue GC formation in PGDs at high redshift, in something of an *ad-hoc* manner. Since this occurs when the gas surface-densities of these PGDs are still high and rapidly forming 'unbound' stars. it begs the question what physical mechanism could possibly halt GC formation so abruptly?

One possibility arises from the cosmic re-ionisation (e.g. see van den Bergh 2001). At some point in the early Universe, gas cooled and began forming stars, providing enough UV flux to ionise the neutral inter-galactic medium (e.g Loeb & Barkana 2001). Recent studies of QSO absorption systems have possibly now constrained the onset of this re-ionisation to be $5 \leq z \leq 6$ (Fan et al. 2000; Becker et al. 2001; Djorgovski et al. 2001). Cen (2001) has suggested that such an external radiation field is sufficient to compress haloes of mass $\leq 10^{7.5} M_{\odot}$, thereby forming self-gravitating baryonic systems, under the proviso that such haloes have low initial angular momentum. By assuming that such systems fragment and form stars, Cen (2001) shows that these stellar systems will have characteristic masses and sizes consistent with metal-poor GCs.

Whilst plausible, this explanation is rather unsatisfactory. Given our current knowledge that GCs are forming in a wide range of star-forming environments, the assertion that the formation of metal-poor GCs is somehow a 'special' process in the early Universe seems somewhat contrived. Perhaps a more self-consistent picture of GC formation is suggested by the study of Larsen & Richtler (2000). These authors found that the efficiency of star cluster formation is a function of the local SFR in spiral discs, implying that the efficiency of GC formation may generically depend upon the rate of star formation in their host galaxy. In this way, GCs may represent the long-lived tracers of the peaks of the cosmic SFR, occurring in relatively un-evolved PGDs at high redshift. Unfortunately, from the standpoint of this study, we found that an $\epsilon \propto$ SFR relation fails to reproduce a metal-poor GC component anything like that observed. This arises because the SFR in our model peaks at $z = 1 \sim 2$, rather than at the required $z > 5$ (i.e. greater than our blue GC truncation redshift).

However, whilst contemporary observations of the cosmic SFR indicate that it reaches a peak at $z \leq 2$ (e.g. see compilation of Blain et al. 1999), its behaviour at higher redshifts ($z > 4$) is relatively unconstrained (Loeb & Barkana 2001). Barkana & Loeb (2000) found from CDM simulations

that the comoving SFR should exhibit a distinct decrease around the re-ionisation redshift (e.g. see their figure 1, for the case of $z_{\rm reion} = 7$). A higher SFR at such redshifts could plausibly give rise to the formation of significant numbers of blue GCs.

6   SUMMARY AND CONCLUSIONS

We have outlined a scheme for forming the globular cluster (GC) systems of elliptical galaxies within the framework of a semi-analytic model of galaxy formation. Our principal results are as follows:

- we can reproduce the observed bimodal colour distributions of GC systems associated with elliptical galaxies by assuming *i)* metal-rich globular clusters are formed during gaseous mergers and *ii)* metal-poor GCs are formed in gaseous proto-galactic discs, and this formation is truncated at $z \sim 5$.
- gaseous mergers which lead to the formation of metal-rich GCs and field stars do not significantly effect the total S_N of the host elliptical galaxy. This remains true even if a relatively high formation efficiency is assumed ($\epsilon_{\rm red} = 0.007$, assuming no dynamical destruction of the GCs occurs.)
- the number of GCs ($N_{\rm GC}$) scales with host galaxy luminosity ($L_{V,\rm gal}$) as $N_{\rm GC} \propto L_{V,\rm gal}^{1.25}$. This arises due to an increasing $\mathcal{M}/\mathcal{L}$ ratio of the simulated ellipticals with luminosity. This is consistent with observations of luminous 'normal' ellipticals, but inconsistent with observations of the highest-S_N galaxies.
- the mean colours of both the metal-rich and metal-poor GCs weakly correlate with the magnitude of the host galaxy, a result is consistent with the current observations.
- the mean colours of the metal-rich GCs are very similar to the mean colours of their host galaxy. The colours of the metal-poor GCs are significantly bluer than their host galaxy, corresponding to a metallicity difference of ~ 1.0 dex. This is consistent with contemporary observations.
- we find that 93% of the simulated GC systems are intrinsically bimodal. However, whether this is 'detected' in broad-band colours is extremely sensitive to sample size, photometric uncertainties, and to a lesser extent, the statistical test employed to detect sub-populations.
- the metal-poor GCs have mean ages of ~ 12 Gyr, whilst the metal-rich GCs have mean ages of ~ 9 Gyr. The age range of the metal-rich GCs in the majority of individual galaxies is large ($5 \sim 12$ Gyr). This age range increases for low-luminosity ellipticals, and for ellipticals in lower mass dark matter haloes.

We have found that by assuming GC formation occurs contemporaneously with unbound star formation, two phases of GC formation are required to produce the observed GC systems of elliptical galaxies. Hierarchical merging at high redshift results in a metal-rich peak consistent with observations, if the metal-rich GC formation efficiency is ~ 0.7 % by stellar mass. Formation of the metal-poor peak requires less efficient (~ 0.2 %) GC formation in low-mass haloes at $z \geq 5$. Models which represent a synthesis of star formation, galaxy formation and cosmology will be required to determine their origin.

The decoupling of the formation of the metal-poor GCs from the galaxy stars at high redshift implies that they are not direct probes of the galaxy star formation. Rather, the metal-poor GCs follow the star formation in relatively un-enriched gas associated with low-mass haloes at early times (e.g. Ashman & Bird 1993). In contrast, the metal-rich GCs directly trace the merger history of their host galaxy whenever star formation occurs. Therefore, the metal-rich GCs are remnants of both star formation at later times, and the dynamical assembly of their host galaxies through merging. We suggest that the metal-rich GCs provide a key to probing the formation epoch of elliptical galaxies.

REFERENCES

Aguilar L., Hut P., Ostriker J. P., 1988, ApJ, 335, 720
Anders E., Grevesse N., 1989, GeCoA, 53, 197
Ashman K. A., Bird C. M., Zepf S. E., 1994, AJ, 108, 2348
Ashman K. M., Bird C. M., 1993a, AJ, 106, 2281
Ashman K. M., Bird C. M., 1993b, in American Astronomical Society Meeting, Vol. 183, p. 7415
Ashman K. M., Zepf S. E., 1992, ApJ, 384, 50
Ashman K. M., Zepf S. E., 1998, Globular cluster systems. Globular cluster systems / Keith M. Ashman, Stephen E. Zepf. Cambridge, U. K. ; New York : Cambridge University Press, 1998. (Cambridge astrophysics series ; 30)
Ashman K. M., Zepf S. E., 2001, astro-ph/0107146
Barkana R., Loeb A., 2000, ApJ, 539, 20
Barmby P., Huchra J. P., Brodie J. P., Forbes D. A., Schroder L. L., Grillmair C. J., 2000, AJ, 119, 727
Barth A. J., Ho L. C., Filippenko A. V., Sargent W. L., 1995, AJ, 110, 1009
Baugh C. M., Cole S., Frenk C. S., 1996, MNRAS, 283, 1361
Baugh C. M., Cole S., Frenk C. S., Lacey C. G., 1998, ApJ, 498, 504
Beasley M. A., Sharples R. M., Bridges T. J., Hanes D. A., Zepf S. E., Ashman K. M., Geisler D., 2000, MNRAS, 318, 1249
Becker R. H., etal. , 2001, astro-ph/0108097
Benson A. J., Cole S., Frenk C. S., Baugh C. M., Lacey C. G., 2000, MNRAS, 311, 793
Binggeli B., Tammann G. A., Sandage A., 1987, AJ, 94, 251
Blain A. W., Jameson A., Smail I., Longair M. S., Kneib J.-P., Ivison R. J., 1999, MNRAS, 309, 715
Blakeslee J. P., 1997, ApJ Lett., 481, L59
Blakeslee J. P., Tonry J. L., Metzger M. R., 1997, AJ, 114, 482
Bower R. G., Lucey J. R., Ellis R. S., 1992, MNRAS, 254, 601
Brodie J. P., Huchra J. P., 1990, ApJ, 362, 503
Brodie J. P., Huchra J. P., 1991, ApJ, 379, 157
Burgarella D., Kissler-Patig M., Buat V. ., 2001, AJ, 121, 2647

Carney B. W., Harris W. E., 2001, "Saas-Fee Advanced Course on Star Clusters". Saas-Fee Advanced Course on Star Clusters Bruce W. Carney / William E. Harris, Swiss Society for Astrophysics and Astronomy, Springer.

Carretta E., Gratton R. G., Clementini G., Fusi Pecci F., 2000, ApJ, 533, 215

Cen R., 2001, ApJ, 560, 592

Cohen J. G., Blakeslee J. P., Ryzhov A., 1998, ApJ, 496, 808

Cole S., Aragon-Salamanca A., Frenk C. S., Navarro J. F., Zepf S. E., 1994, MNRAS, 271, 781

Cole S., Lacey C. G., Baugh C. M., Frenk C. S., 2000, MNRAS, 319, 168

Cote P., Marzke R. O., West M. J., 1998, ApJ, 501, 554

di Fazio A., Capuzzo Dolcetta R., 1987, AAP, 184, 263

Djorgovski S., Santiago B. X., 1992, ApJ Lett., 391, L85

Djorgovski S. G., Castro S. M., Stern D., Mahabal A., 2001, astro-ph/0108069

Durrell P. R., Harris W. E., Geisler D., Pudritz R. E., 1996, AJ, 112, 972

Elmegreen B. G., Efremov Y. N., 1997, ApJ, 480, 235

Elson R. A. W., Santiago B. X., Gilmore G. F., 1996, New Astronomy, 1, 1

Fan X. et al., 2000, AJ, 120, 1167

Forbes D. A., Beasley M. A., Brodie J. P., Kissler-Patig M., 2001, ApJ Lett., 563, L143

Forbes D. A., Brodie J. P., Grillmair C. J., 1997, AJ, 113, 1652

Forbes D. A., Brodie J. P., Huchra J., 1997, AJ, 113, 887

Forbes D. A., Brodie J. P., Larsen S. . S., 2001, ApJ Lett., 556, L83

Forbes D. A., Forte J. C., 2001, MNRAS, 322, 257

Forbes D. A., Franx M., Illingworth G. D., Carollo C. M., 1996, ApJ, 467, 126

Forbes D. A., Hau G. K. T., 2000, MNRAS, 312, 703

Forte J. C., Geisler D., Ostrov P. G., Piatti A. ., Gieren W., 2001, AJ, 121, 1992

Gebhardt K., Kissler-Patig M., 1999, AJ, 118, 1526

Geisler D., Lee M. G., Kim E., 1996, AJ, 111, 1529

Gnedin N. Y., Ostriker J. P., 1997, ApJ, 486, 581

Haehnelt M. G., Steinmetz M., Rauch M., 1998, ApJ, 495, 647

Harris W. E., 1996, AJ, 112, 1487

Harris W. E., Harris G. L. H., McLaughlin D. E., 1998, AJ, 115, 1801

Harris W. E., van den Bergh S., 1981, AJ, 86, 1627

Hartigan J. A., Hartigan P. M., 1985, Ann. Stat., 13, 70

Holtzman J. A. et al., 1992, AJ, 103, 691

Kauffmann G., 1996, MNRAS, 281, 487

Kauffmann G., Charlot S., 1998, MNRAS, 294, 705

Kauffmann G., White S. D. M., Guiderdoni B., 1993, MNRAS, 264, 201

Kissler-Patig M., 1997, AAP, 319, 83

Kissler-Patig M., Brodie J. P., Schroder L. L., Forbes D. A., Grillmair C. J., Huchra J. P., 1998, AJ, 115, 105

Kodama T., Arimoto N., Barger A. J., Arag'on-Salamanca A., 1998, AAP, 334, 99

Kundu A., Whitmore B. C., 2001, AJ, 121, 2950

Kurth O. M., Fritze-v. Alvensleben U., Fricke K. J., 1999, AAPS, 138, 19

Larsen S. . S., Brodie J. P., Huchra J. P., Forbes D. A., Grillmair C. J., 2001, AJ, 121, 2974

Larsen S. S., Richtler T., 1999, AAP, 345, 59

Larsen S. S., Richtler T., 2000, AAP, 354, 836

Lee M. G., Kim E., 2000, AJ, 120, 260

Lee M. G., Kim E., Geisler D., 1998, AJ, 115, 947

Loeb A., Barkana R., 2001, ARA&A, 39, 19

Ma J., Shu C. G., 2001, MNRAS, 322, 927

Maller A. H., Somerville R. S., Prochaska J. X., Primack J. R., 1999, in After the Dark Ages: When Galaxies were Young (the Universe at $2 < z < 5$). 9th Annual October Astrophysics Conference in Maryland held 12-14 October, 1998. College Park, Maryland. Edited by S. Holt and E. Smith. American Institute of Physics Press, 1999, p. 102, p. 102

McLaughlin D. E., 1999, AJ, 117, 2398

McLaughlin D. E., Pudritz R. E., 1996, ApJ, 457, 578

Meurer G. R., Heckman T. M., Leitherer C., Kinney A., Robert C., Garnett D. R., 1995, AJ, 110, 2665

Mihos J. C., Hernquist L., 1996, ApJ, 464, 641

O'Connell R. W., 1976, ApJ, 206, 370

O'Connell R. W., Gallagher J. S., Hunter D. A., 1994, ApJ, 433, 65

Ostrov P. G., Forte J. C., Geisler D., 1998, AJ, 116, 2854

Prochaska J. X., Wolfe A. M., 1997, ApJ, 487, 73

Prochaska J. X., Wolfe A. M., 1998, ApJ, 507, 113

Puzia T. H., Kissler-Patig M., Brodie J. P., Huchra J. P., 1999, AJ, 118, 2734

Rood H. J., Dickel J. R., 1978, ApJ, 224, 724

Schweizer F., 2001, in IAU Symposia, Vol. 207

Schweizer F., Miller B. W., Whitmore B. C., Fall S. M., 1996, AJ, 112, 1839

Secker J., Geisler D., McLaughlin D. E., Harris W. E., 1995, AJ, 109, 1019

Somerville R. S., Primack J. R., 1999, MNRAS, 310, 1087

van den Bergh S., 1975, ARA&A, 13, 217

van den Bergh S., 2001, astro-ph/0108298

Vesperini E., 2000, MNRAS, 318, 841

Watson A. M. et al., 1996, AJ, 112, 534

West M. J., Cote P., Jones C., Forman W., Marzke R. O., 1995, ApJ Lett., 453, L77

White S. D. M., Frenk C. S., 1991, ApJ, 379, 52

White S. D. M., Rees M. J., 1978, MNRAS, 183, 341

Whitmore B. C., Schweizer F., 1995, AJ, 109, 960

Whitmore B. C., Zhang Q., Leitherer C., Fall S. M., Schweizer F. ., Miller B. W., 1999, AJ, 118, 1551

Wolfe A. M., 1988, in Proceedings of the QSO Absorption Line Meeting, p. 297

Worthey G., 1994, ApJS, 95, 107

Zepf S. E., Ashman K. M., 1993, MNRAS, 264, 611

Zepf S. E., Ashman K. M., English J., Freeman K. C., Sharples R. M., 1999, AJ, 118, 752

Zepf S. E., Ashman K. M., Geisler D., 1995, ApJ, 443, 570

Zepf S. E., Geisler D., Ashman K. M., 1994, ApJ Lett., 435, L117